

A Sustainable Strategy for Visible-light driven facile N-formylation of amines Using Co(II) embedded Covalent organic framework as an efficient photocatalyst

Surya Das,^a Priyanka Sarkar,^a Manoj Goswami,^b Sk. Murshed Ali,^c Mijanur Rahaman Mollah^c and Sk. Manirul Islam^{*,a}

^aDepartment of Chemistry, University of Kalyani, Kalyani, Nadia, 741235, W.B., India.

^bCSIR-Advanced Materials and Processes Research Institute (AMPRI), Bhopal 462026, India

^cDepartment of Chemistry, University of Calcutta, Acharya Prafulla Chandra Road, Kolkata 700009, W.B., India

*Email: manir65@rediffmail.com

Contents

1. Materials	Page S3
2. Instrumentation.....	Page S3-S4
3. Figure S1. ¹³ C solid state NMR.....	Page S4
4. Figure S2. Image of reaction set-up	Page S5
5. Figure S3. Preparation of 2,4,6-Triformylphloroglucinol (Tp)	Page S5-S6
6. Figure S4: Preparation of 2,4,6- tris(hydrazino)-1,3,5-triazine (TH).....	Page S6
7. Figure S5. BET analysis of Tp-TH COF support	Page S7
8. Figure S6. TGA-DTA plot of Co(II)@Tp-TH COF catalyst.....	Page S7
9. Figure S7. (a) XPS spectrum of the synthesized Tp- COF.....	Page S8
10. Figure S8. Electron image and EDAX analysis of Tp-TH COF support.....	Page S8
11. Figure S9. (a) Solid state UV-vis spectroscopy and Tauc plot Tp-TH COF....	Page S9
12. Figure S10. Kinetic curve for the reaction.....	Page S9
13. Figure S11. Comparison of conversion rates for different recycling runs.....	Page S10
14. Figure S12. PXRD pattern of the reused Co(II)@Tp-TH Catalyst.....	Page S10
15. Figure S13. FT IR spectra of the reused Co(II)@Tp-TH Catalyst.....	Page S11

16. Figure S14. FE-SEM and HR-TEM image of reused photocatalyst....	PageS11-S12
17. Figure S16. EDAX of reused Co(II)@Tp-TH Catalyst.....	Page S12
18. Figure S17. XPS spectra reused Co(II)@Tp-TH COF photocatalyst after 5 th run.....	Page S13
19. Figure S18. ¹ H NMR spectra of 2,4,6-triformylphloroglucinol (Tp).....	Page S13
20. Figure S19-S40. ¹ H and ¹³ C NMR spectra of Products.....	Page S14-S42
21. References.....	Page S42

Materials

Phloroglucinol, hexamethylenetetramine (HMTA) and cyanuric chloride were received from Sigma Aldrich, India. Hydrazine, trifluoroacetic acid and cobalt acetate tetrahydrate were purchased from TCI, India. 1,4 dioxane, acetone, tetrahydrofuran (THF), chloroform, N, N-dimethylformamide (DMF), mesitylene and methanol were obtained from Merck, India and used without further purification. All other reagents and solvents were bought from E-Merk, India and were used as received. The CO₂ gas cylinder was acquired from Apollo Engineering Gas Service, India. All the reactions were performed under atmospheric CO₂ using oven-dried Schlenk balloon set-up technique.

Instrumentation

Absorption spectroscopy: UV-vis absorption spectra of the catalyst was recorded on SHIMADZU, UV-2600 UV-vis spectrometer with a standard 1 cm x 1 cm cuvette.

NMR Spectra: ¹H NMR (Proton nuclear magnetic resonance spectra) were performed on a Bruker 400 MHz spectrometer. Chemical shifts for protons are reported in parts per million (ppm).

PXRD: The PXRD analysis of the photocatalyst (Co(II)@Tp-TH COF) was executed by using an X-ray diffractometer (BRUKER, Powder X-Ray ecoD8 ADVANCE) equipped with Ni-filtered Cu K α (λ = 0.15406 nm) radiation.

IR Spectra: The FTIR spectra of the synthesized and starting materials were conducted by using a Perkin-Elmer spectrophotometer (FT-IR 783) on KBr Pellets.

FESEM: FESEM images of the catalyst were acquired by using Scanning Electron Microscope (SEM) [JEOL JSM IT 300], which helps to know about the morphological information of the sample.

TEM: Transmission Electron Microscope (TEM) [JEOL JEM 2100] was used to get the morphological information of the sample.

TGA:The thermal stability of the Co(II)@Tp-TH COF material was analysed by a Thermogravimetric Analyzer [Model: Perkin Elmer-Pyris-Diamond, TG/DTA] at the rate of 10 °C per min up to 800 °C in presence of air.

BET:The N₂ adsorption-desorption analysis of Co(II)@Tp-TH sample was conducted by using a BET Surface Analyzer [QUANTACHROME ASIQC602-5].

Fluorescence Spectroscopy:The Fluorescence Emission spectra was recorded by using Horiba Fluoro Max 4 spectrometer.

CHN Analysis: A CHNOS elemental analyser (Vario EL III) was performed to find out the contents of C, N and H in Co(II)@Tp-TH catalyst.

EIS analysis: The measurements have been performed in 0.1 M PBS solution and a conventional three-electrode system where Co(II)@Tp-TH catalyst on the glassy carbon electrode is used as the working electrode and double junction Ag/AgCl saturated with 3.0M KCl is used as a reference electrode. The Platinum wire served as a counter electrode. The electrochemical impedance spectroscopy (EIS) has been carried out in the frequency range of 100 kHz -0.01 Hz with an AC amplitude of 10 mV at a constant the applied potential of 5 mV.

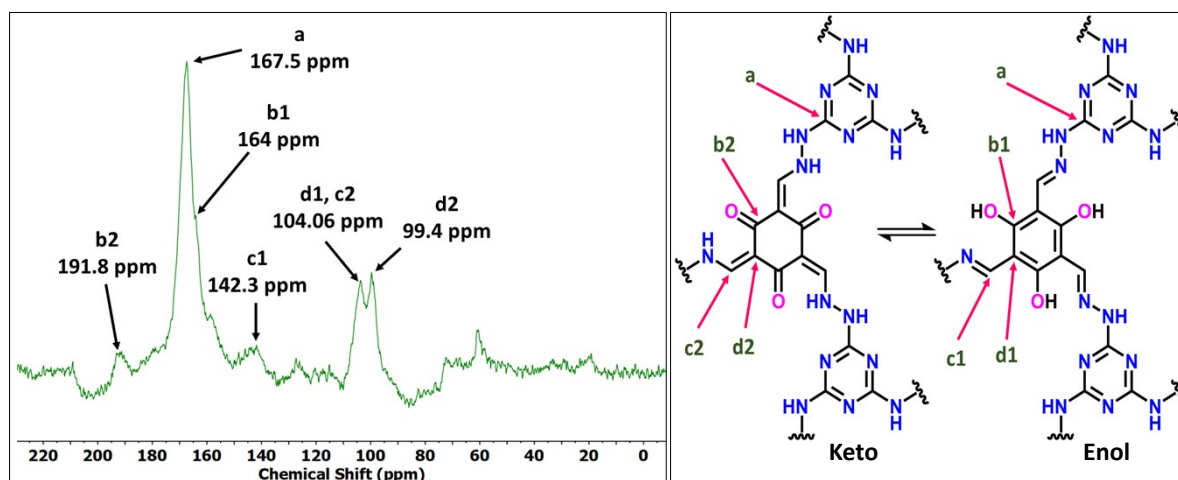


Figure S1. ¹³C solid state NMR of Tp-TH COF.

As described in Figure S1, peaks from both keto and enol forms are present in the structure of the COF powder. A comparative depiction is displayed here for better understanding (Figure S1). ^{13}C solid state NMR suggests that the synthesized COF material consists of keto and enol forms. The C signal at 191.8 ppm for the carbonyl carbon of the keto form and the carbon signal at 167.5 ppm for the triazine unit. In keto form, the peaks positioned at 104.6 and 99.8 ppm are ascribed to the carbon centres being present in the $-\text{NH}-\text{C}=\text{C}$ bond. Additionally, the chemical shift value at 142.3 and 104.06 ppm are related to the carbon atoms of the $-\text{N}=\text{C}-\text{C}$ bond in enol form. All these data provided adequate chemical composition evidence for the successful preparation of Tp-TH 2D COF.

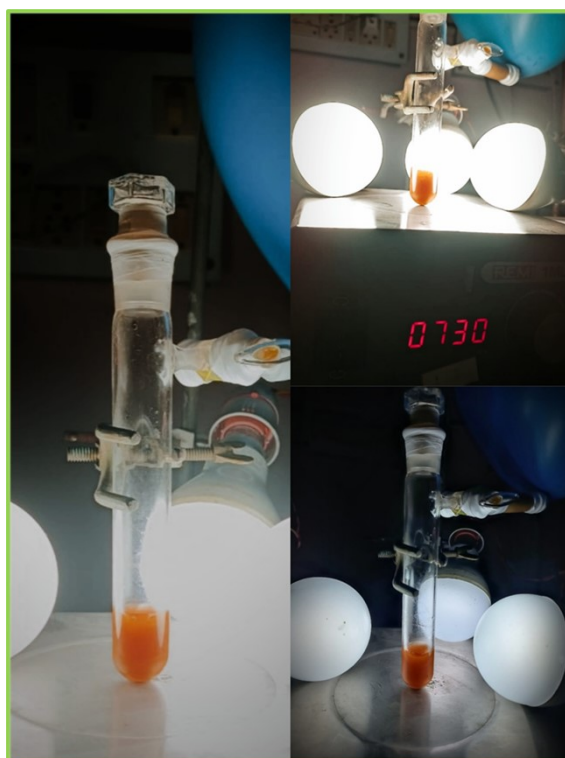


Figure S2: Image of reaction set-up under 20 W White LED for one-pot N-formylation reaction of amines.

Preparation of the catalyst

Schematic presentation for the synthesis of the covalent organic framework-supported cobalt catalyst ($\text{Co(II)}@\text{Tp-TH}$) is shown in Scheme 3 in the manuscript.

General procedure for the production of 2,4,6-Triformylphluroglucinol (Tp)

Synthesis of 2,4,6-Triformylphloroglucinol (Tp) was prepared according to the preceding literature.¹In a brief, trifluoroacetic acid (90 mL), hexamethylene tetramine (108 mmol) and dried phloroglucinol (49 mmol) were taken in a 500 ml round bottom flask and heated at 100°C for 2.5 h under N₂ atmosphere. Approximately 150 ml of 3M hydrochloric acid was added very carefully to the resulting solution under continuous magnetic stirring at fixed temperature for next 1 h. After cooling to room temperature, the solution was extracted with DCM and dried over anhydrous Na₂SO₄. The obtained extract was concentrated to yield dull yellow coloured solid and the crude solid was further purified by hot ethanol to yield desired product (Tp).

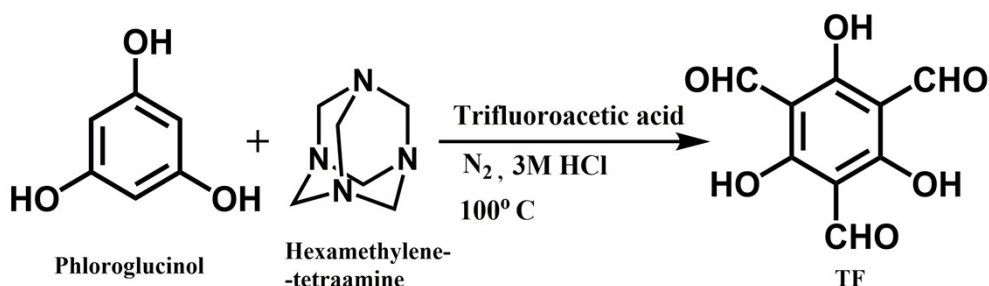


Figure S3:Preparation of 2,4,6-Triformylphloroglucinol (Tp)

General procedure for the production of 2,4,6-Trihydrazino-1,3,5-triazine (TH)

2,4,6-Trihydrazino-1,3,5-triazine(TH) was synthesized according to the previous literatures.^{2,3} Hydrazine (1 mL, 18 mmol) was dissolved in 1,4-dioxane (5 mL) in a round bottom flask. Then, a solution containing cyanuric chloride (2.99 mmol) in 1,4-dioxane (5 mL) was added dropwise to the previous solution with a continuous stirring bar over 1 h. It was left for further 2 h stirring at room temperature. Then, it was allowed to reach the reflux conditions for 8 h. The resulting product was separated by filtration and washed with distilled water and 1,4-dioxane, respectively and dried at 70 °C under vacuum for 12 h. This product was briefly named TH (yield 82%).

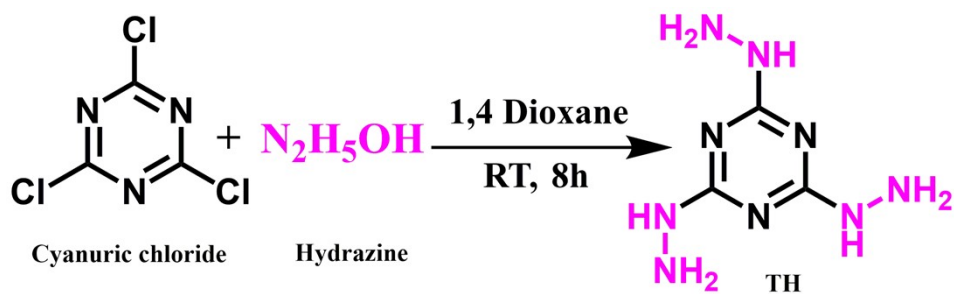


Figure S4: Preparation of 2,4,6- tris(hydrazino)-1,3,5-triazine (TH)

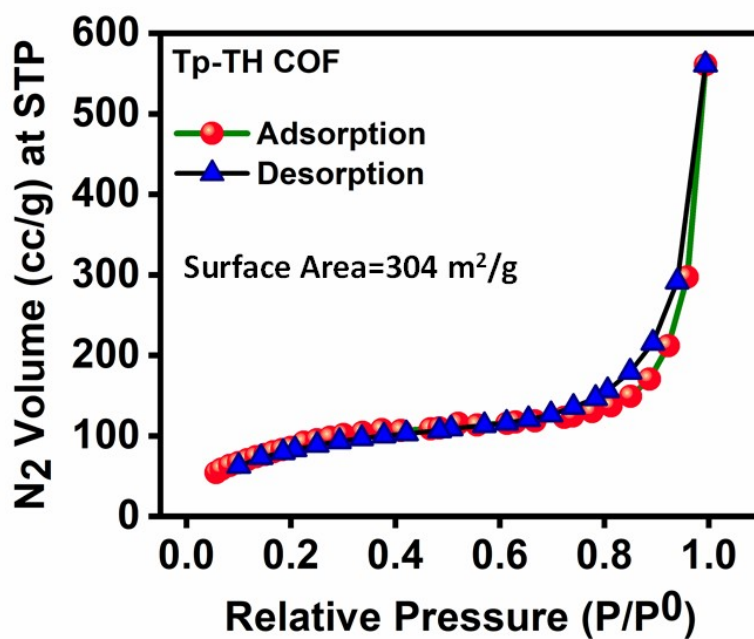


Figure S5. BET isotherm analysis of Tp-TH COF support.

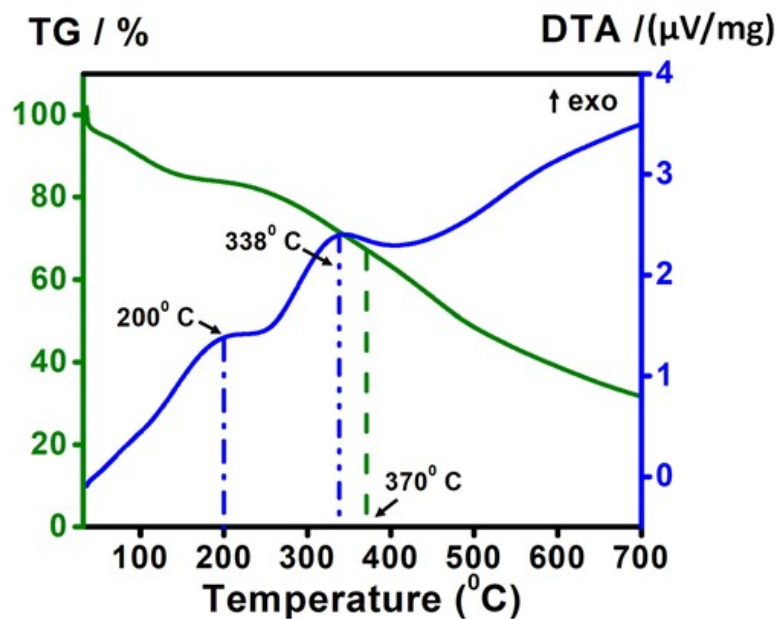


Figure S6. TGA-DTA plot of Co(II)@Tp-TH COF catalyst.

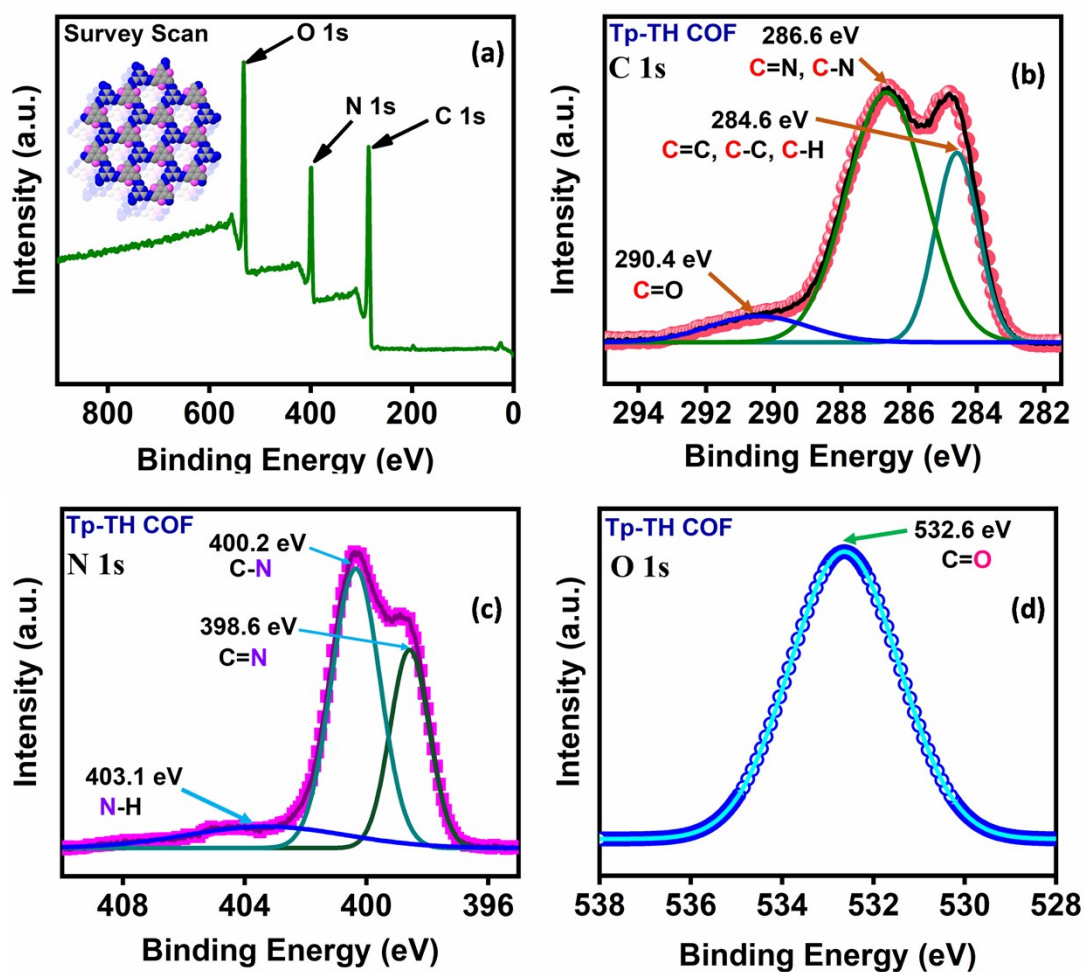


Figure S7. (a) Full-scale XPS survey and deconvoluted (b) C 1s, (c) N 1s, (d) O 1s spectrum of the synthesized Tp-TH COF.

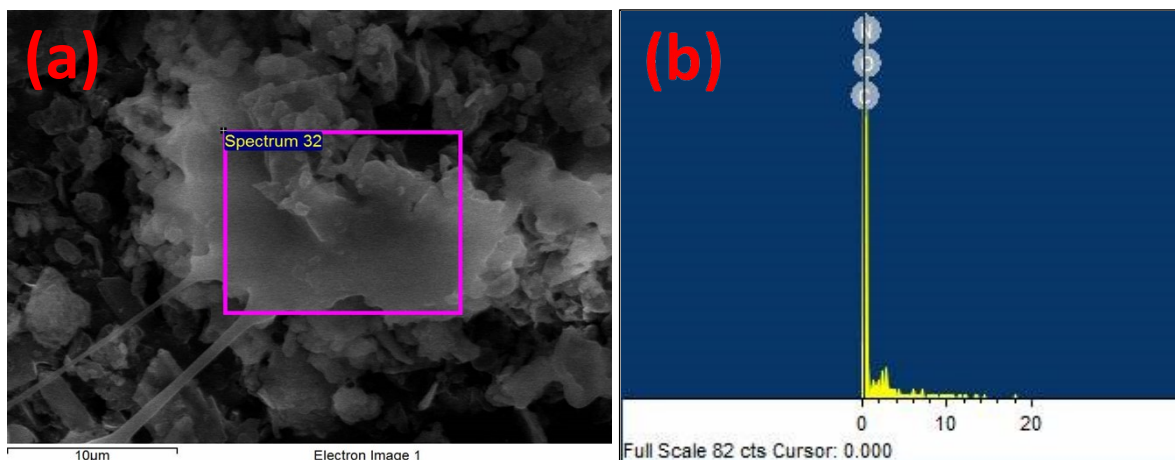


Figure S8. (a) Electron image and (b) EDAX analysis of Tp-TH COF support.

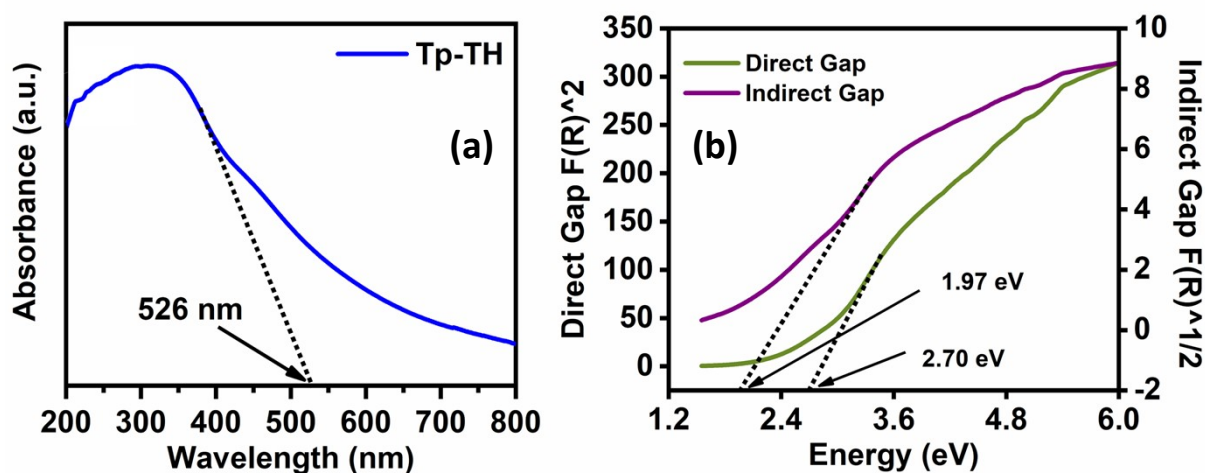


Figure S9.(a) Solid state UV-vis spectroscopy of Tp-TH COF (b) Tauc plot assuming direct and indirect band gap based on absorbance spectroscopy of Tp-TH COF.

Kinetic curve (conversion vs. time) for the reaction:

We have examined the rate of conversion for the reactions with time in presence of the catalyst [Co(II)@Tp-TH] and the kinetic curve has been plotted from the acquired data (Figure S3).

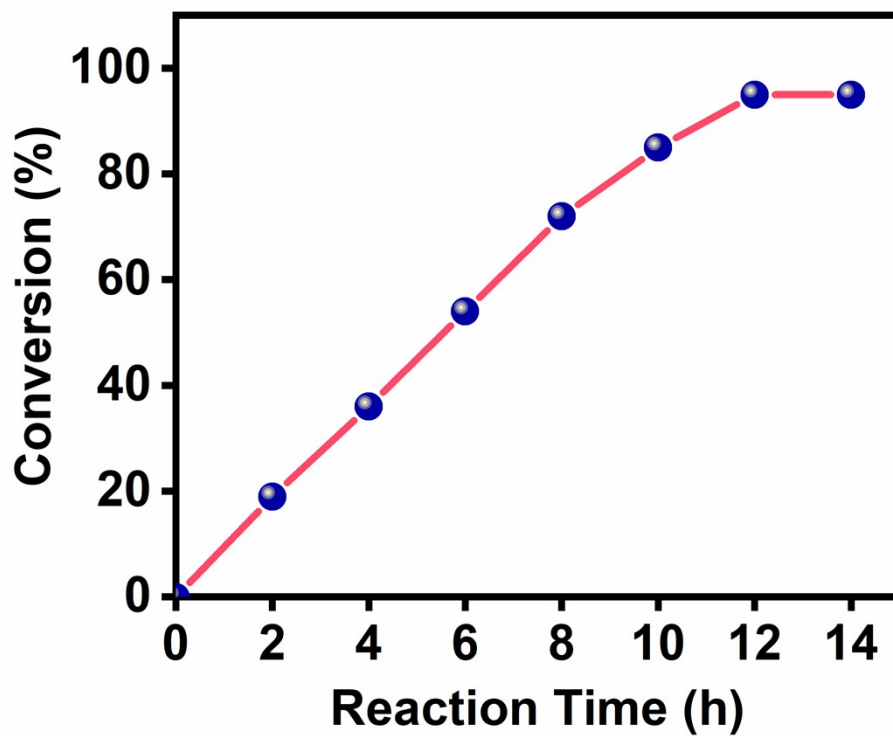


Figure S10. Kinetic curve for the synthesis of N-benzyl formamide.

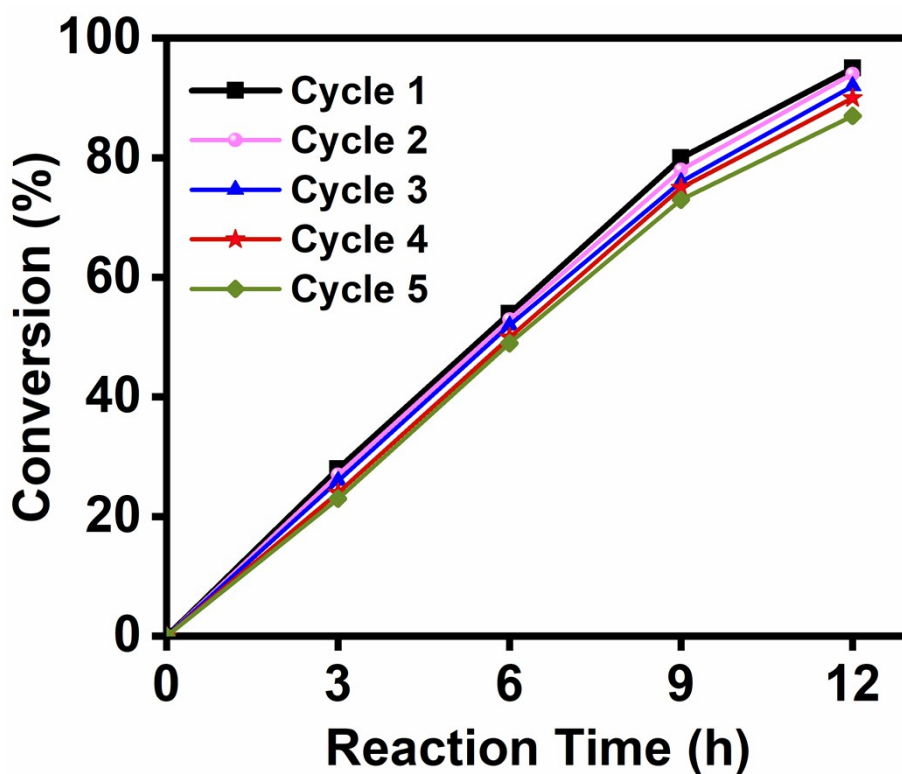


Figure S11. Comparison of conversion rates for different recycling runs (upto 5 cycles).

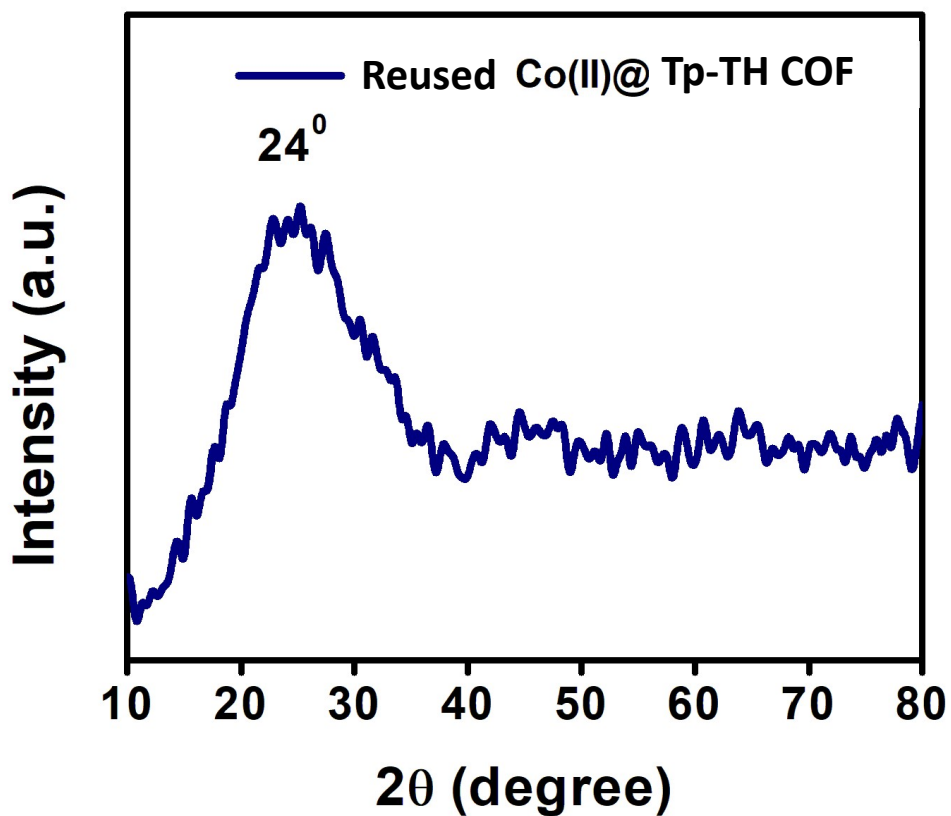


Figure S12. PXRD pattern (Wide angle) of the reused Co(II)@Tp-TH Catalyst.

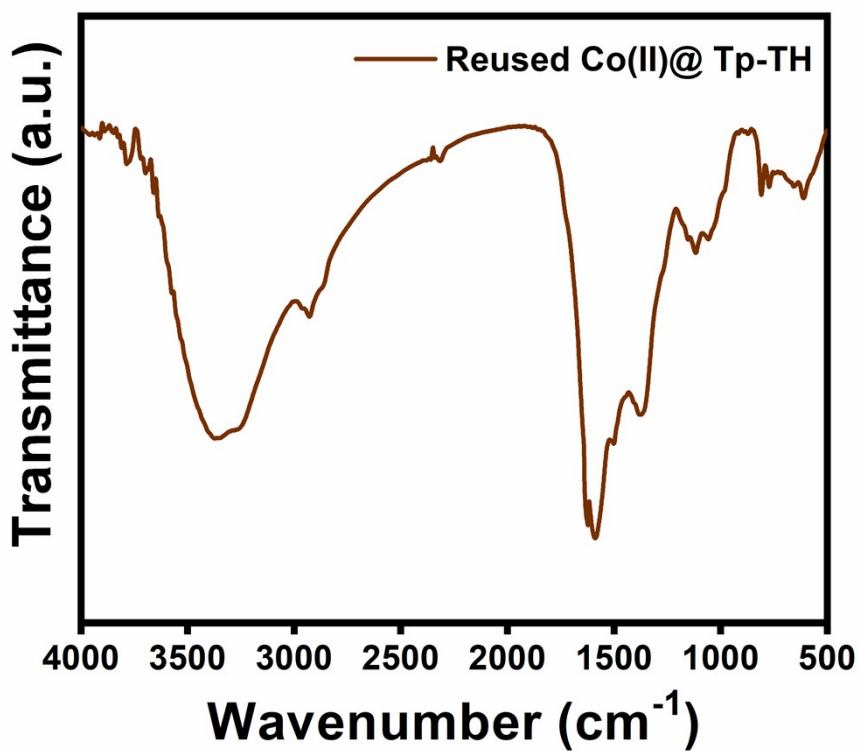


Figure S13. FT IR spectra of the reused Co(II)@Tp-TH Catalyst.

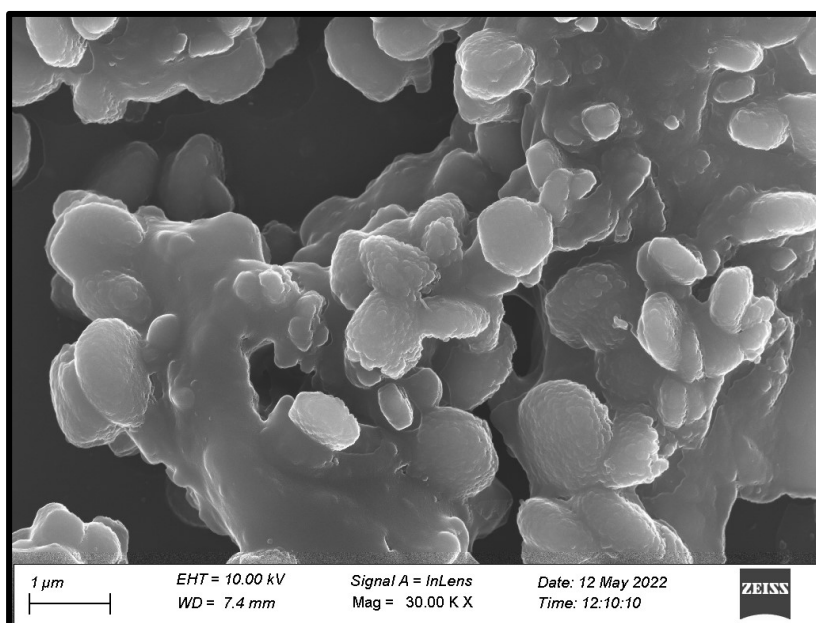


Figure S14. FE-SEM image of reused Co(II)@Tp-TH Catalyst.

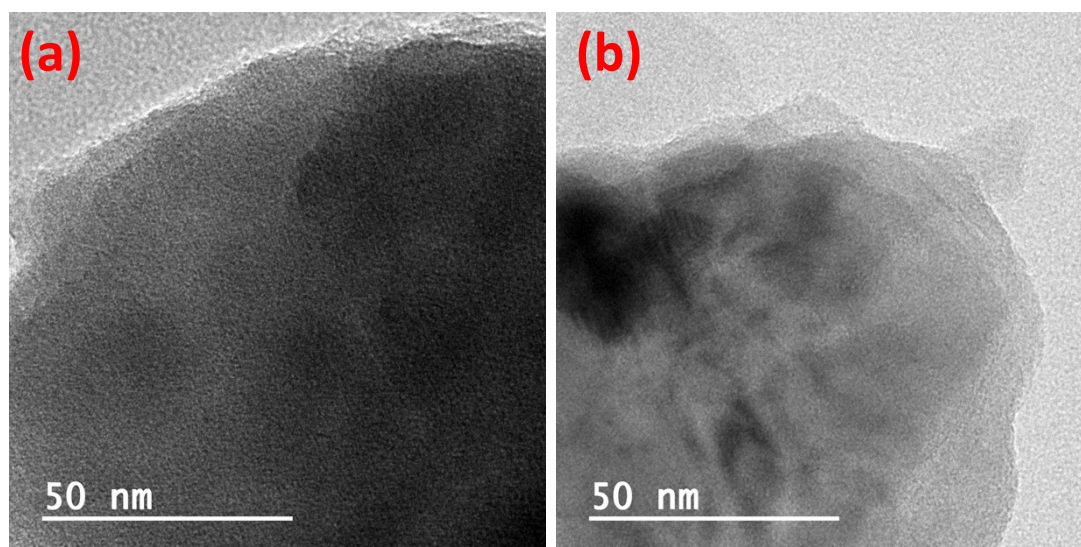


Figure S15. HR-TEM image of reused Co(II)@Tp-TH Catalyst.

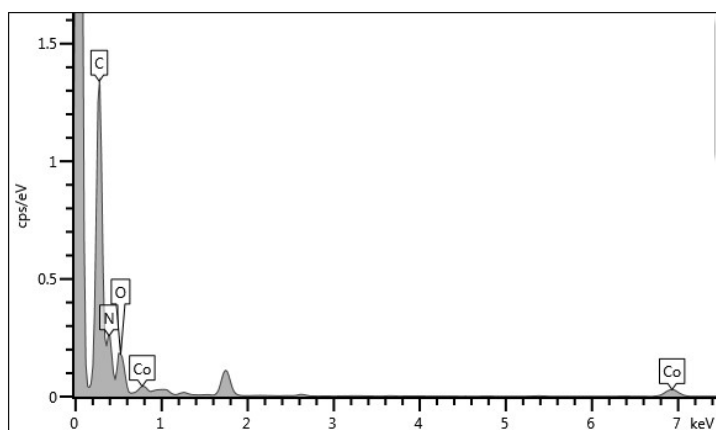


Figure S16. EDAX of reused Co(II)@Tp-TH Catalyst.

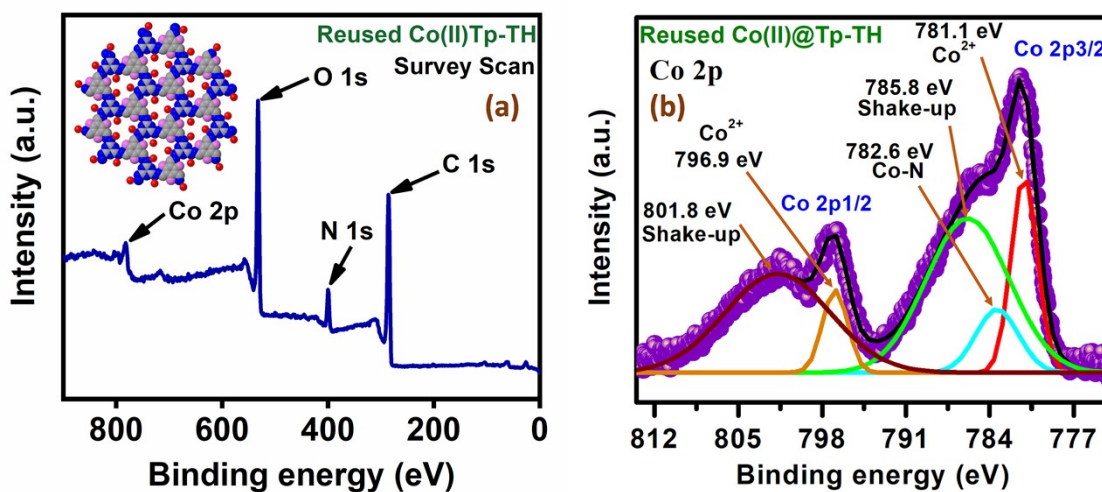


Figure S17. (a) Full-scale XPS survey and (b) deconvoluted Co 2p of the reused Co(II)@Tp-TH COF photocatalyst after 5th run.

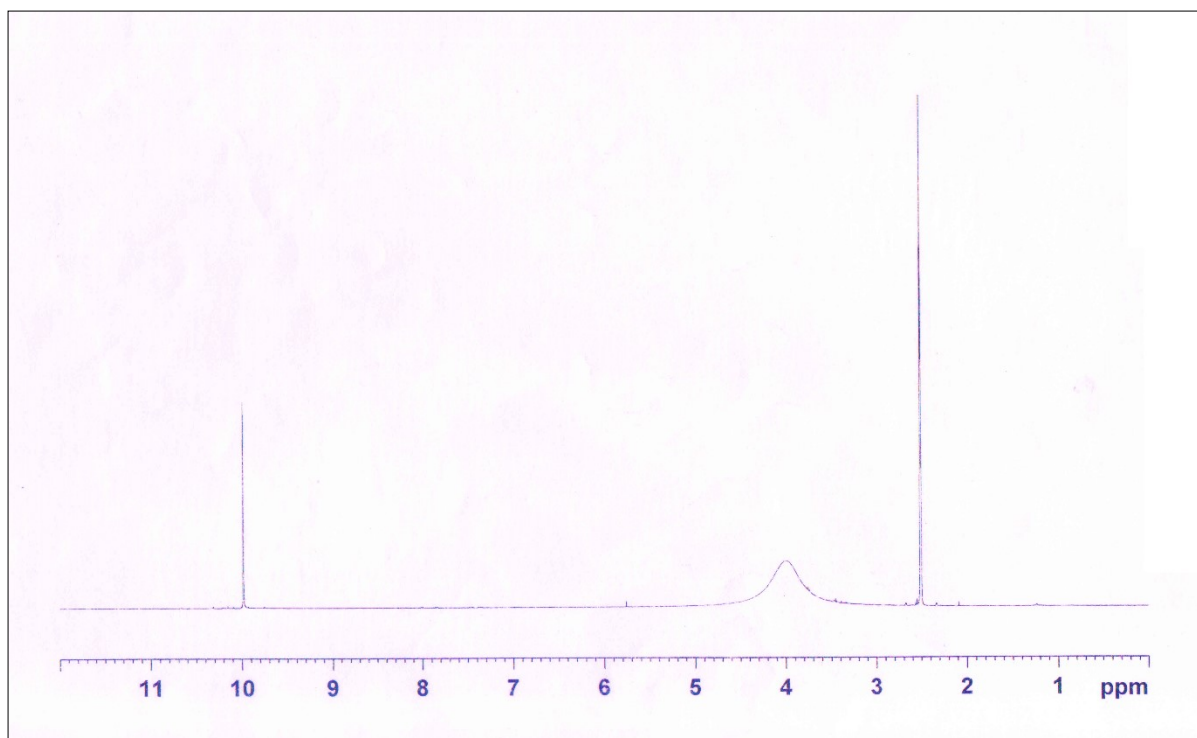
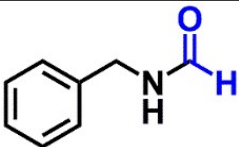
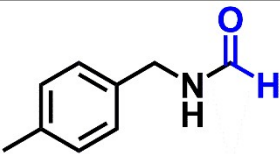
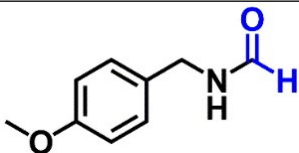
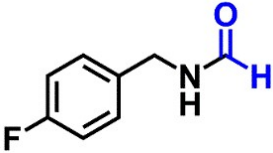
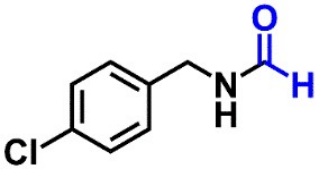
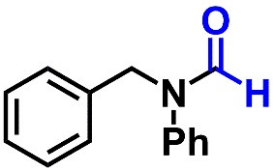
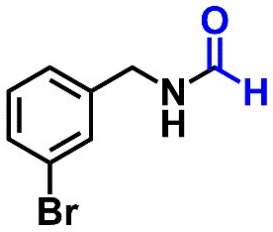
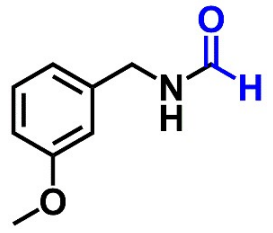
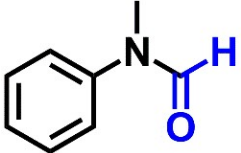
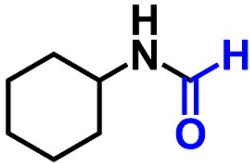
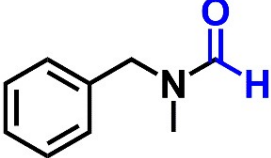
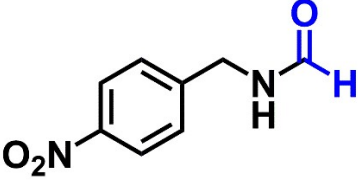
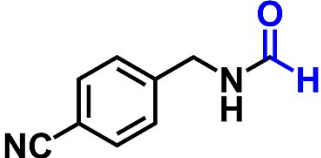
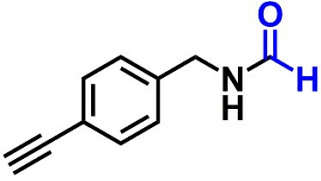


Figure S18. ^1H NMR spectra of 2,4,6-triformylphloroglucinol (Tp)

^1H and ^{13}C NMR data of N-formylated amine derivatives⁴:

	<p>N-benzyl formamide, ^1H NMR (400 MHz, CDCl_3), δ (ppm): 8.093 (s, 1H), 7.115-7.281 (m, 5H), 4.682 (d, $J=1.2$ Hz, 2H). ^{13}C NMR (100 MHz, CDCl_3): δ 42.08, 126.98, 127.07, 127.59, 127.70, 128.73, 128.91, 137.69, 162.26.</p>
	<p>N-(4-methylbenzyl) formamide, ^1H NMR (400 MHz, CDCl_3), δ (ppm): 8.099 (s, 1H), 7.00-7.129 (m, 4H), 5.781 (brs, 1H), 4.299 (d, $J=5.6$ Hz, 2H), 2.245 (s, 3H). ^{13}C NMR (100 MHz, CDCl_3): δ 21.32, 41.61, 127.91, 129.21, 129.39, 134.89, 136.38, 161.81.</p>
	<p>N-(4-methoxybenzyl) formamide, ^1H NMR (400 MHz, CDCl_3), δ (ppm): 8.142 (s, 1H), 6.843-7.205 (m, 4H), 4.576 (d, $J=4.4$ Hz, 2H), 3.724 (s, 3H). ^{13}C NMR (100 MHz, CDCl_3): δ 41.10, 55.61, 114.35, 129.85, 132.10, 158.81, 163.72.</p>

	<p>N-(4-fluorobenzyl) formamide, ^1H NMR (400 MHz, CDCl_3), δ (ppm): 8.191 (s, 1H), 7.103–7.185 (m, 4H), 4.602 (d, $J=6$ Hz, 2H). ^{13}C NMR (100 MHz, CDCl_3): δ 43.02, 115.53, 129.37, 132.34, 160.78, 163.21.</p>
	<p>N-(4-chlorobenzyl) formamide, ^1H NMR(400MHz,CDCl_3)δ(ppm): 8.103(s,1H),7.243-7.270(m, 4H), 6.116 (brs, 1H), 4.627 (d, $J= 0.8$ Hz, 2H). ^{13}C NMR (100 MHz, CDCl_3): δ 41.41, 128.64, 130.92, 133.41, 136.17, 161.30.</p>
	<p>N-phenyl-N-benzyl formamide, ^1H NMR(400MHz,CDCl_3)δ(ppm): 8.59(s,1H),6.724-7.496(m, 10H), 4.924 (d, $J=1.2$ Hz, 2H). ^{13}C NMR (100 MHz, CDCl_3): δ 48.32, 126.33, 126.90, 127.31, 127.61, 128.76, 129.40, 136.15, 139.74, 160.83.</p>
	<p>N-(3-bromobenzyl) formamide, ^1H NMR (400 MHz, CDCl_3), δ (ppm): 8.123 (d, 1H), 6.846-7.825 (m, 4H), 4.637 (d, $J=0.8$ Hz, 2H). ^{13}C NMR (100 MHz, CDCl_3): δ 41.45, 122.97, 126.31, 130.13, 130.90, 131.55, 141.27, 161.15.</p>
	<p>N-(3-methoxybenzyl) formamide, ^1H NMR (400 MHz, CDCl_3), δ (ppm): 8.042 (s, 1H),6.754-7.178 (m, 4H), 4.257 (d, $J=6$ Hz, 2H), 3.706 (s, 3H). ^{13}C NMR (100 MHz, CDCl_3): δ 41.87, 55.32, 111.14, 112.46, 119.86, 129.66, 139.45, 159.90, 162.24.</p>
	<p>N-methyl-N-phenylformamide, ^1H NMR (400 MHz, CDCl_3) δ (ppm): 8.398 (s, 1H), 7.084-7.356 (m, 5H), 3.24 (s, 3H). ^{13}C NMR (100 MHz, CDCl_3): δ 29.67, 122.05, 127.23, 128.22, 144.39, 161.79.</p>
	<p>N-cyclohexyl formamide, ^1H NMR (400 MHz, CDCl_3)δ (ppm): 8.020 (s, 1H), 6.067(s,1H), 3.783 (m, 1H), 1.153-1.863(m, 10H). ^{13}C NMR (100 MHz, CDCl_3): δ 24.74, 25.60, 33.00, 47.08, 160.41.</p>

	<p>N-methyl-N-benzyl formamide, ^1H NMR (400MHz, CDCl_3)δ(ppm): 8.060(s,1H),7.053-7.216(m, 5H), 4.364 (d,J= 0.8 Hz, 2H), 3.474 (s, 3H). ^{13}C NMR (100 MHz, CDCl_3): δ 34.06, 53.50, 127.11, 128.00, 128.51, 136.04, 162.78.</p>
	<p>N-(4-nitrobenzyl) formamide, ^1H NMR (400MHz)δ(ppm): 8.022(s,1H),8.282-8.260 (d, J= 8.8 Hz, 2H), 7.799-7.778 (d,J= 8.4 Hz, 2H), 4.18 (d, J= 1.6 Hz, 2H). ^{13}C NMR (100 MHz): δ 42.33, 121.33, 128.53, 144.91, 146.23, 163.79.</p>
	<p>N-(4-cyanobenzyl) formamide, ^1H NMR (400MHz,CDCl_3)δ(ppm): 8.308(s,1H),7.759-7.739 (d, J= 8, 2H), 7.482-7.455(d, J= 10.8, 2H), 4.222 (d, J= 1.6 Hz, 2H). ^{13}C NMR (100 MHz, CDCl_3): δ 41.87, 110.97, 118.87, 128.47, 128.75, 132.82, 132.88, 144.30, 161.06.</p>
	<p>N-(4-ethynylbenzyl) formamide, ^1H NMR (400MHz,CDCl_3)δ(ppm): 8.012(s,1H),7.545-7.484(m, 4H), 4.044 (d, J= 2 Hz, 2H), 3.026 (s, 1H). ^{13}C NMR (100 MHz, CDCl_3): δ 41.80, 81.95, 83.49, 122.25, 129.68, 132.32, 135.29, 161.55.</p>

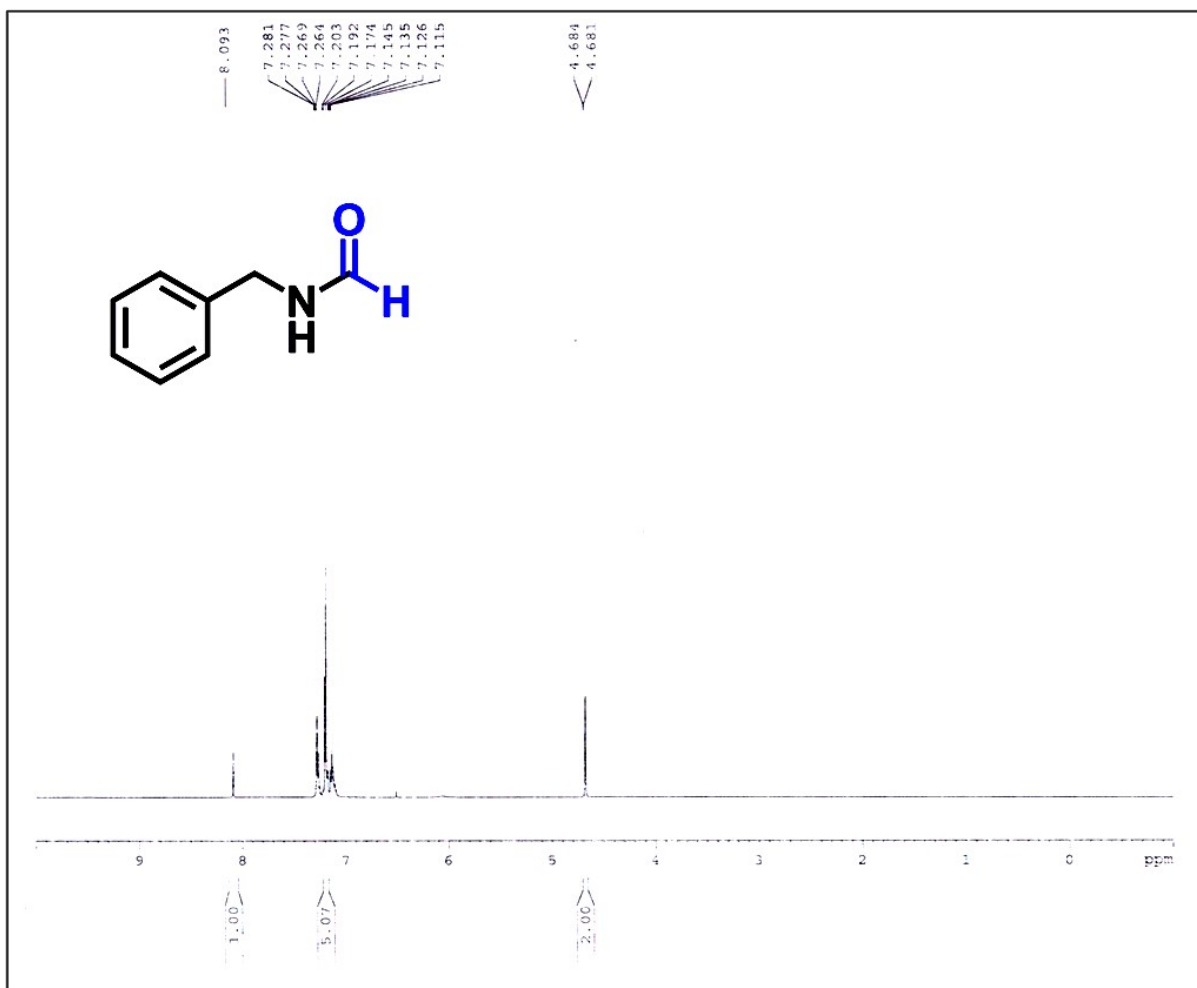


Figure S19: ¹H NMR data of N-benzyl formamide

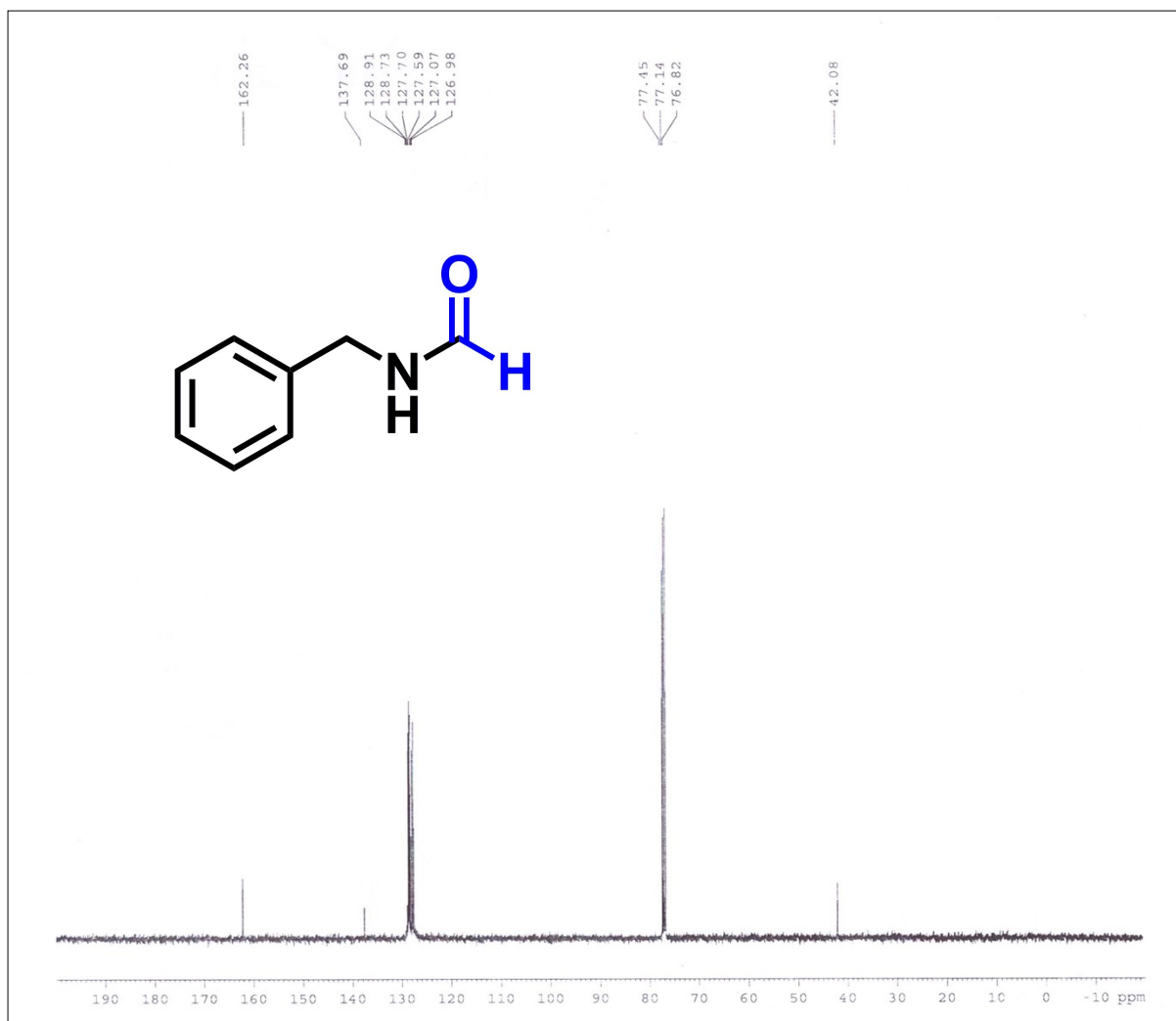


Figure S20: ¹³C NMR data of N-benzyl formamide

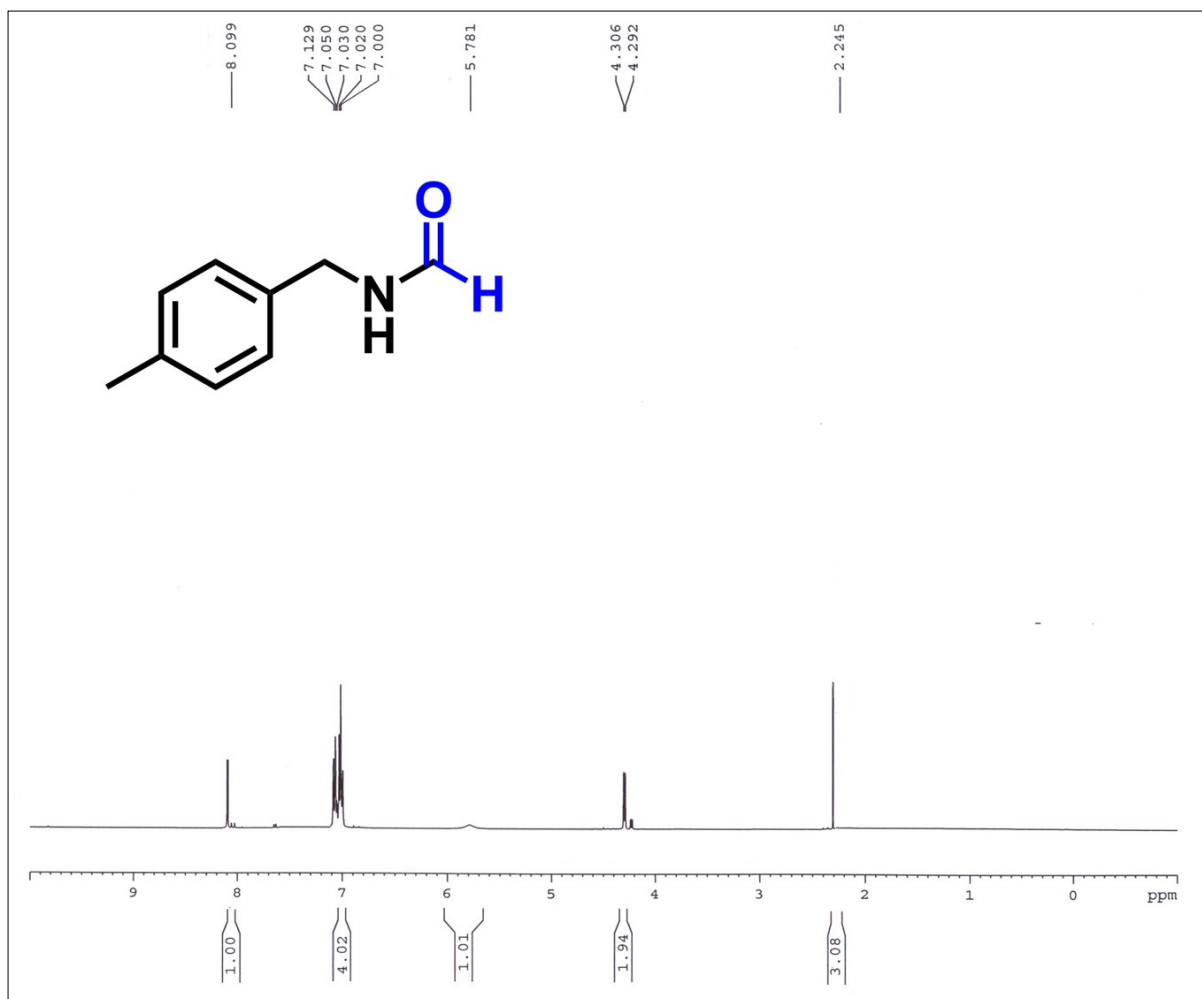


Figure S21: ^1H NMR data of N-(4-methylbenzyl) formamide

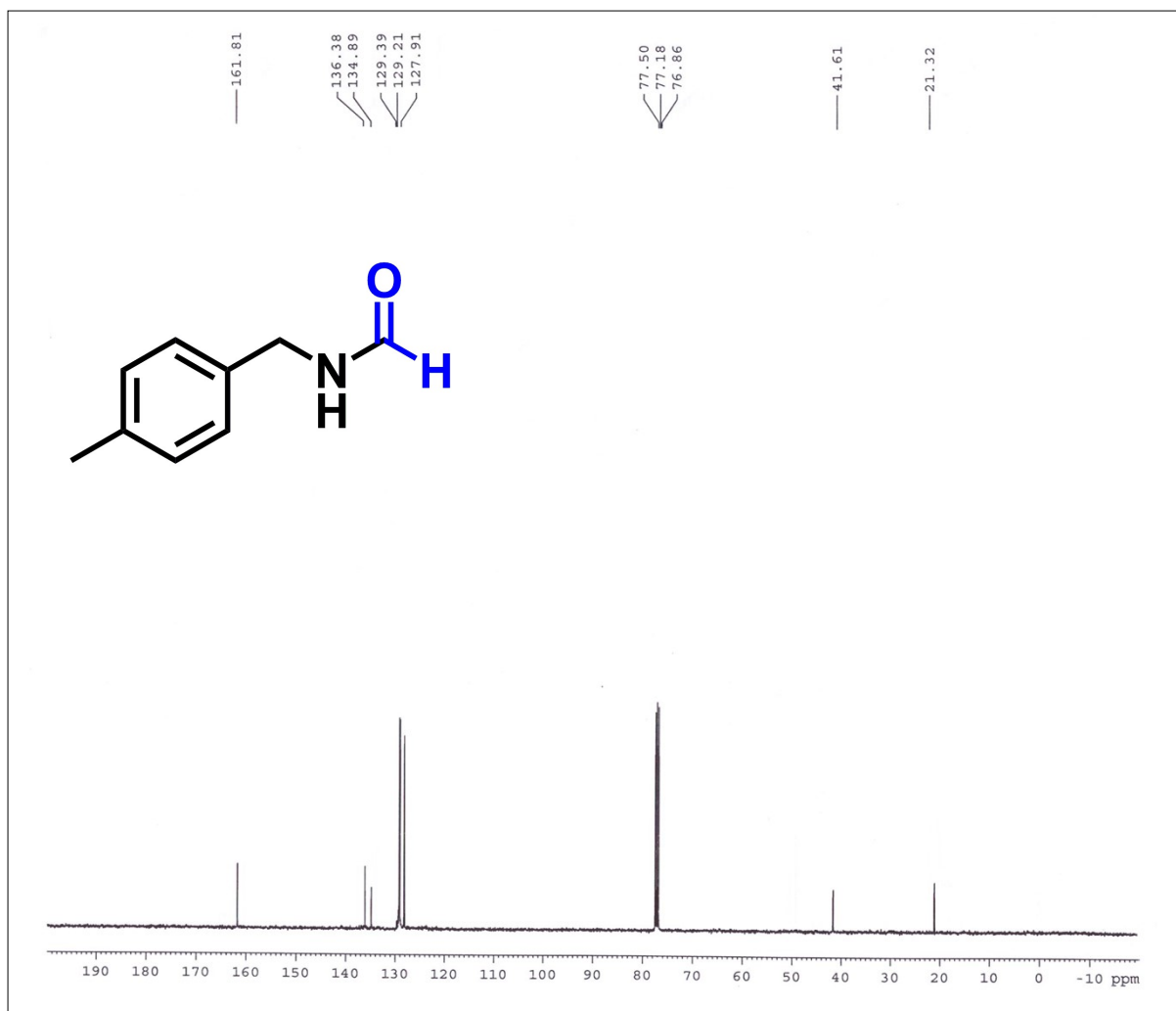


Figure S22: ¹³C NMR data of N-(4-methylbenzyl) formamide

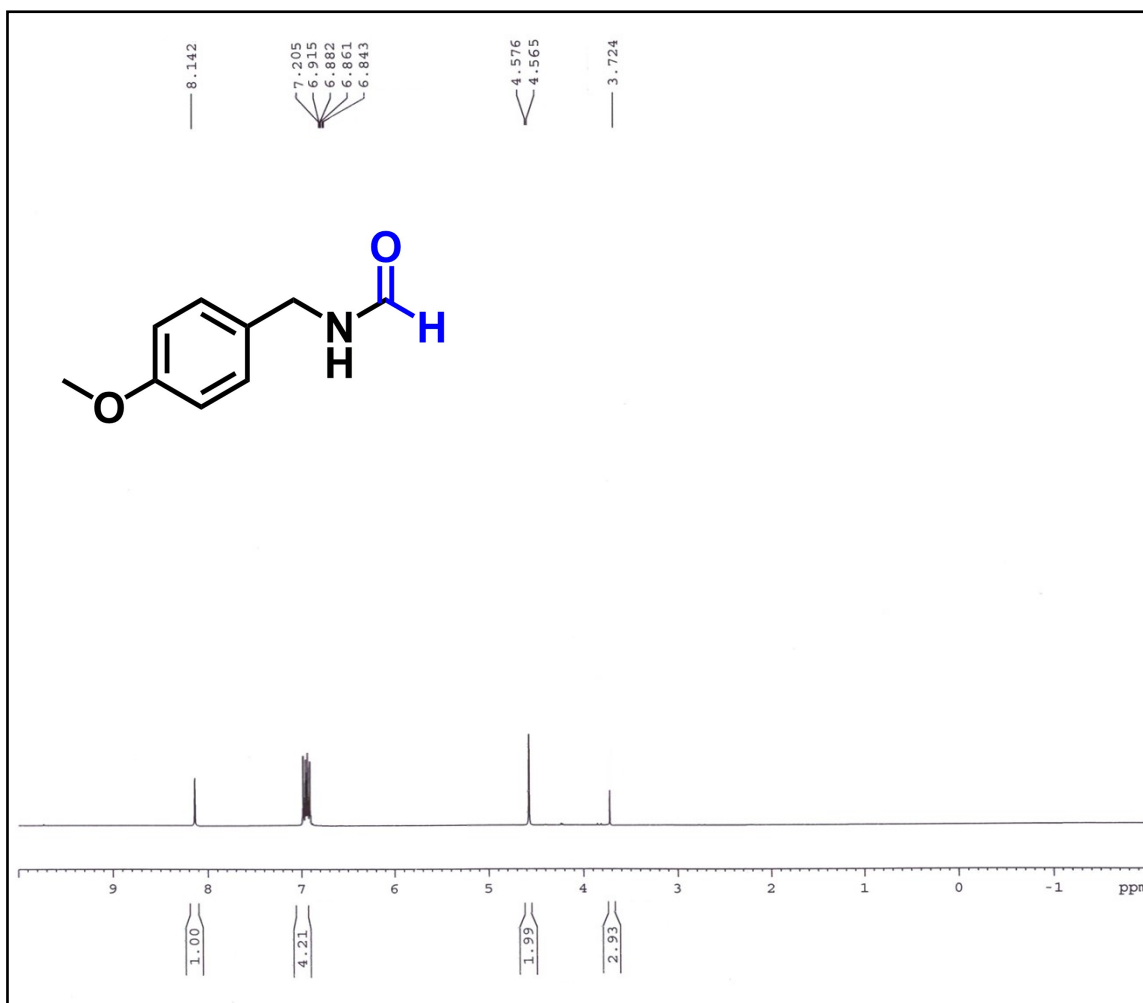


Figure S23: ¹H NMR data of N-(4-methoxybenzyl) formamide

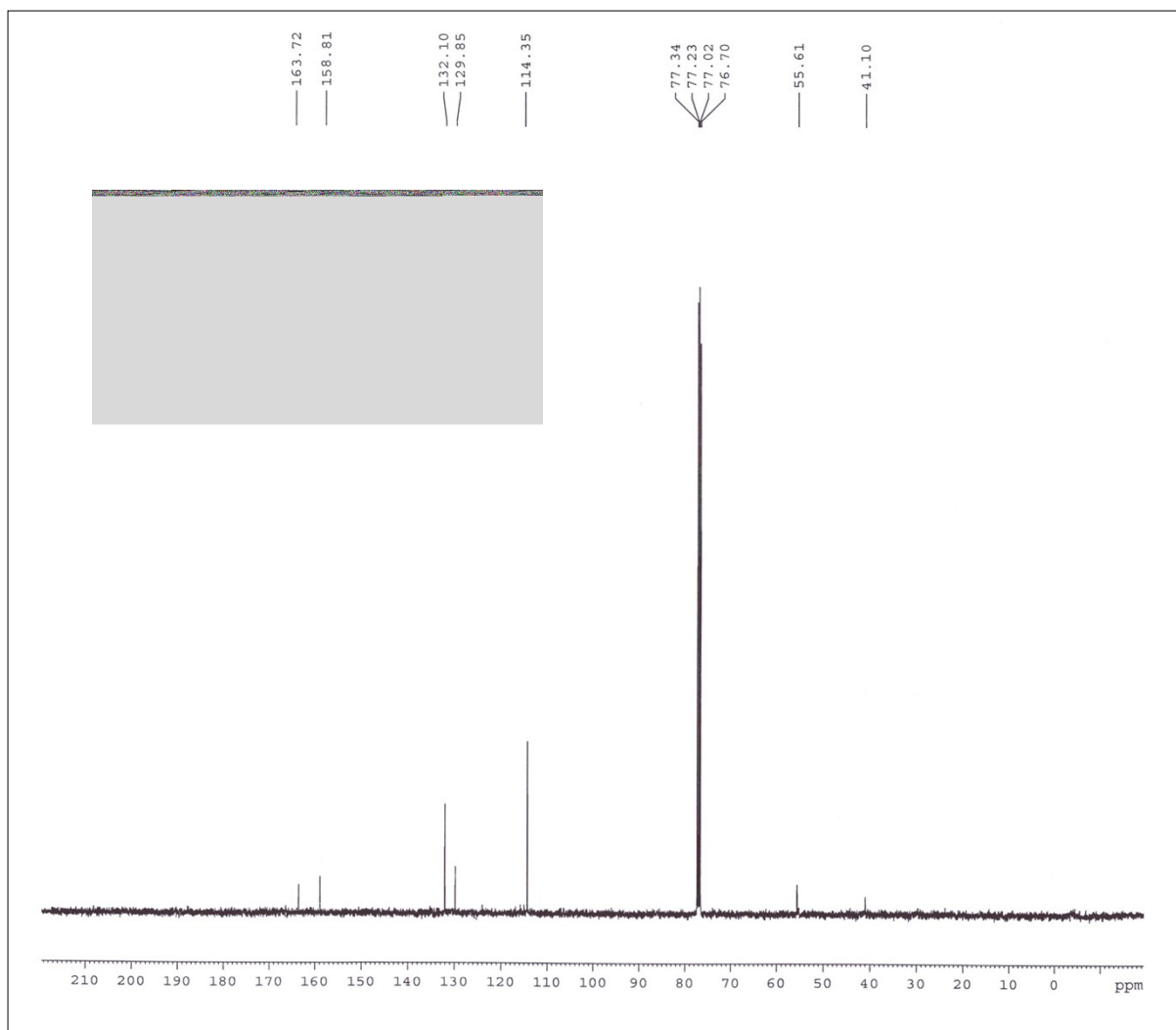


Figure S24: ^{13}C NMR data of N-(4-methoxybenzyl) formamide

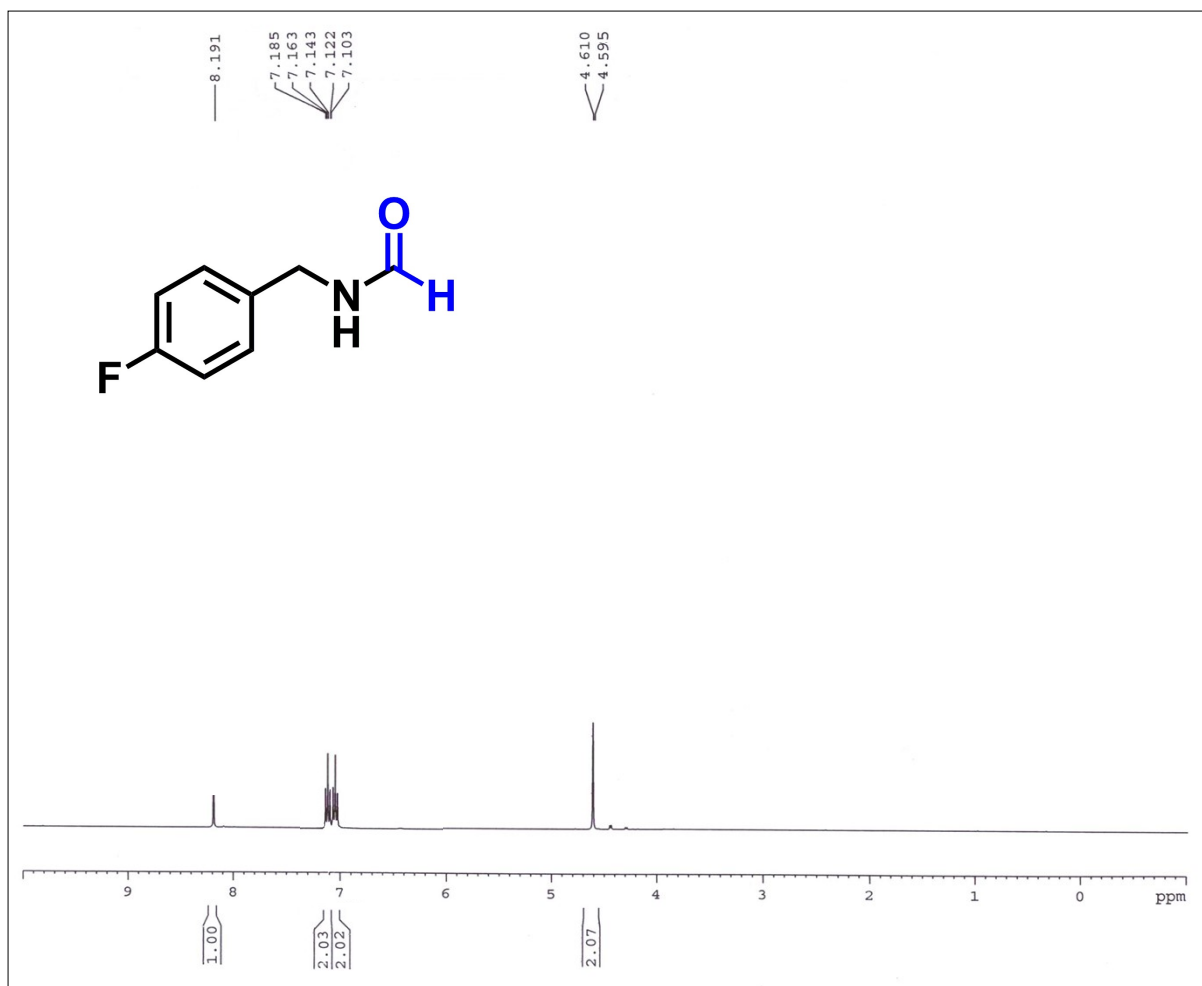


Figure S25: ¹H NMR data of N-(4-fluorobenzyl) formamide

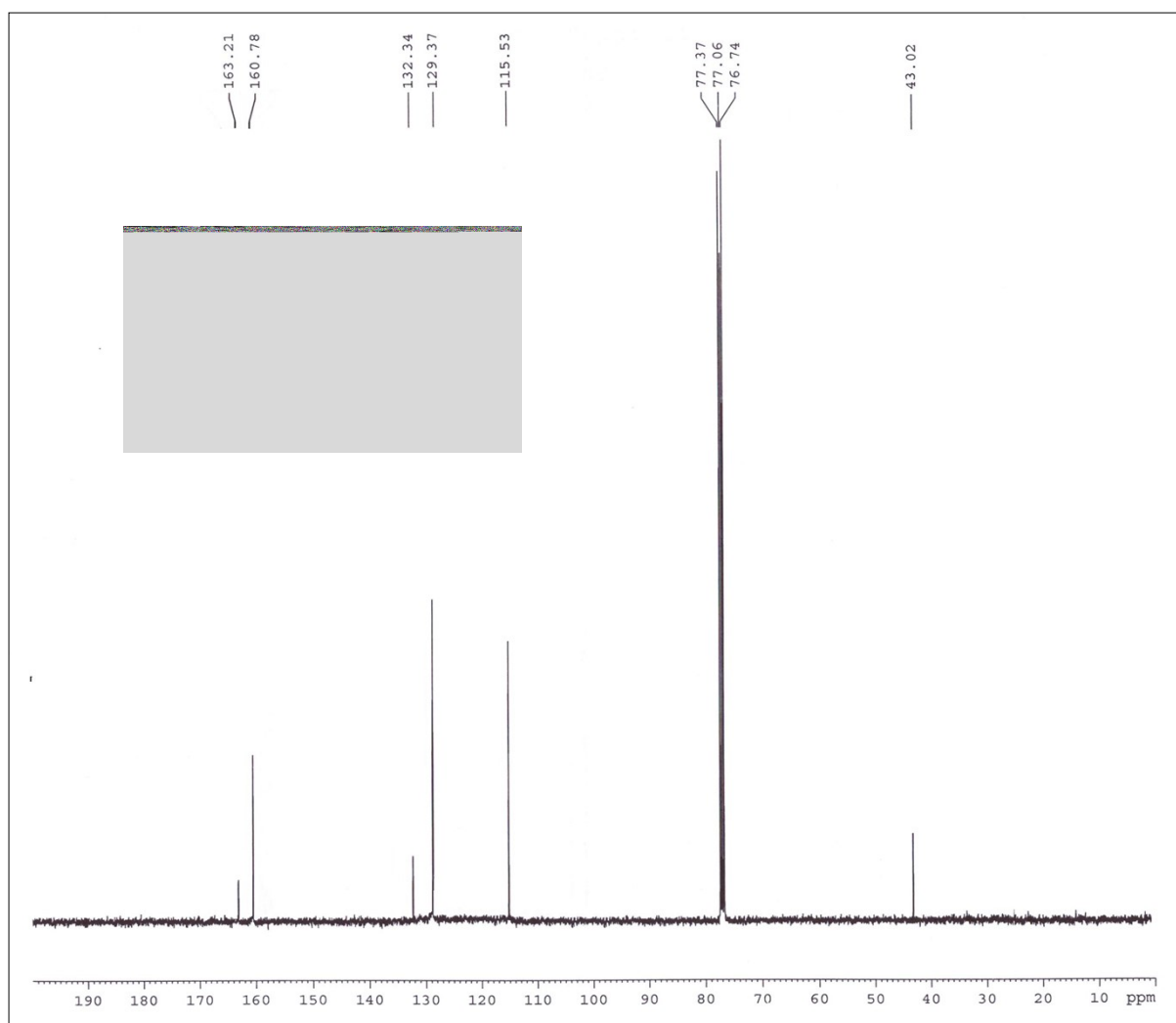


Figure S26: ^{13}C NMR data of N-(4-fluorobenzyl) formamide

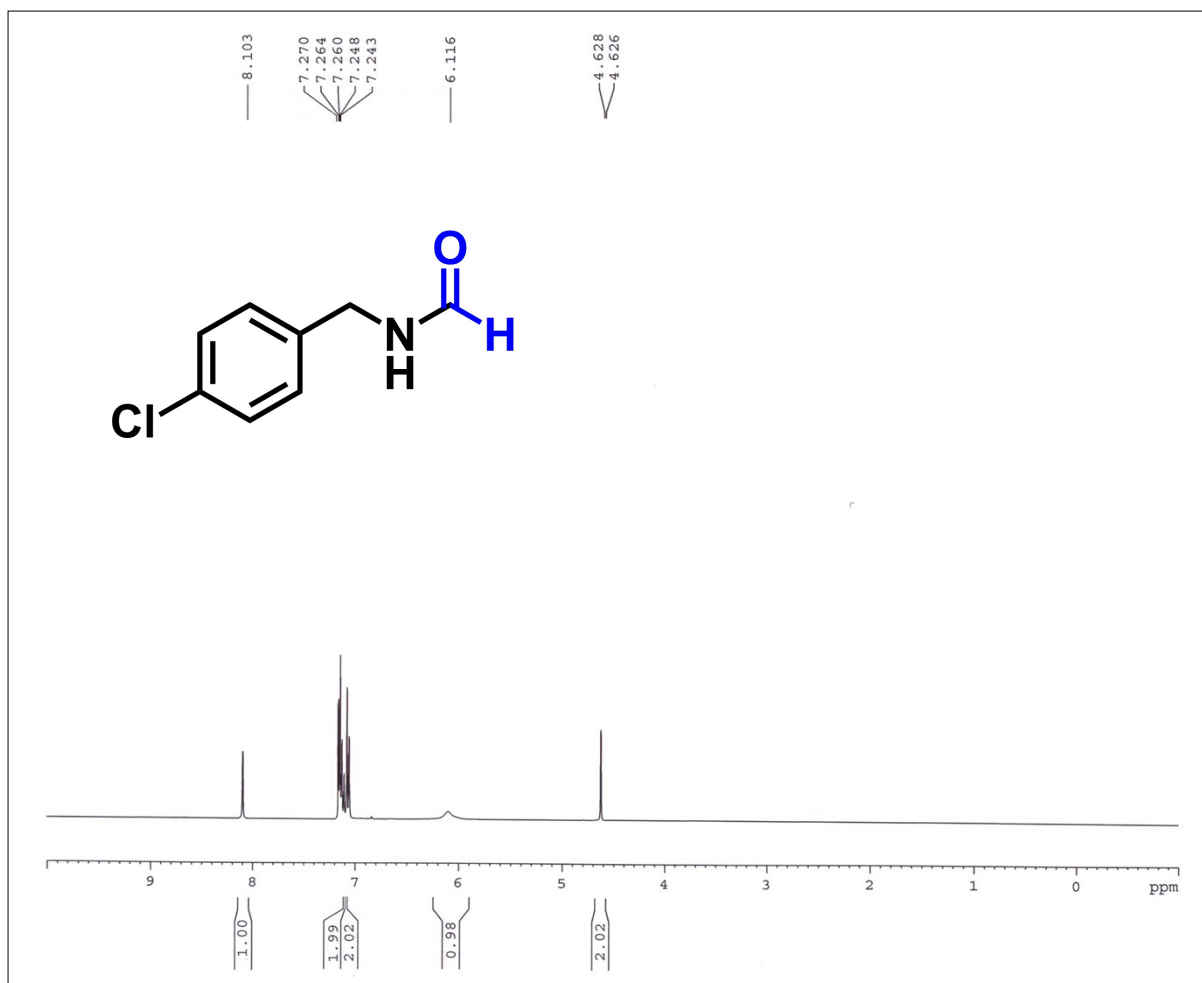


Figure S27: ¹H NMR data of N-(4-chlorobenzyl) formamide

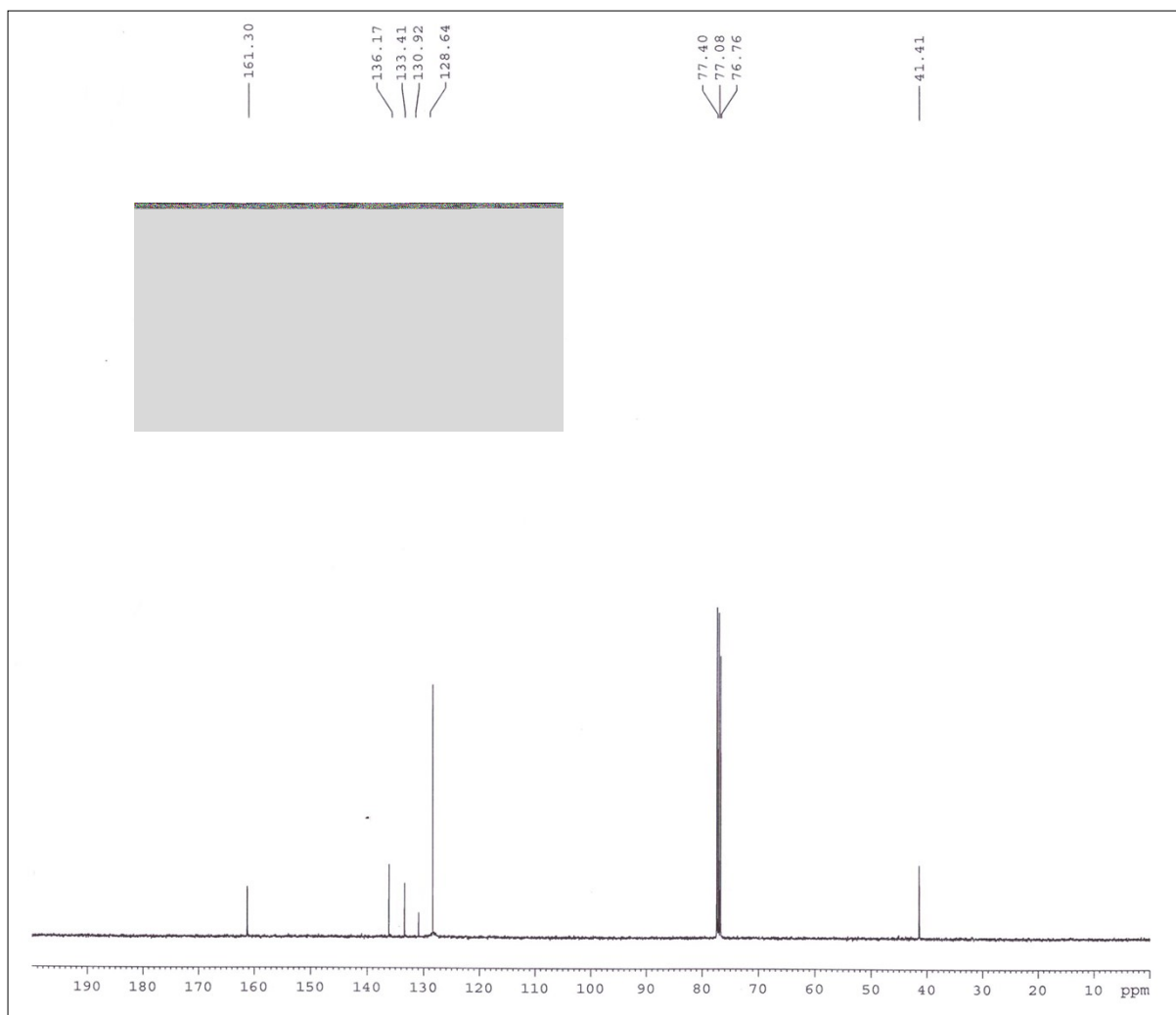


Figure S28: ^{13}C NMR data of N-(4-chlorobenzyl) formamide

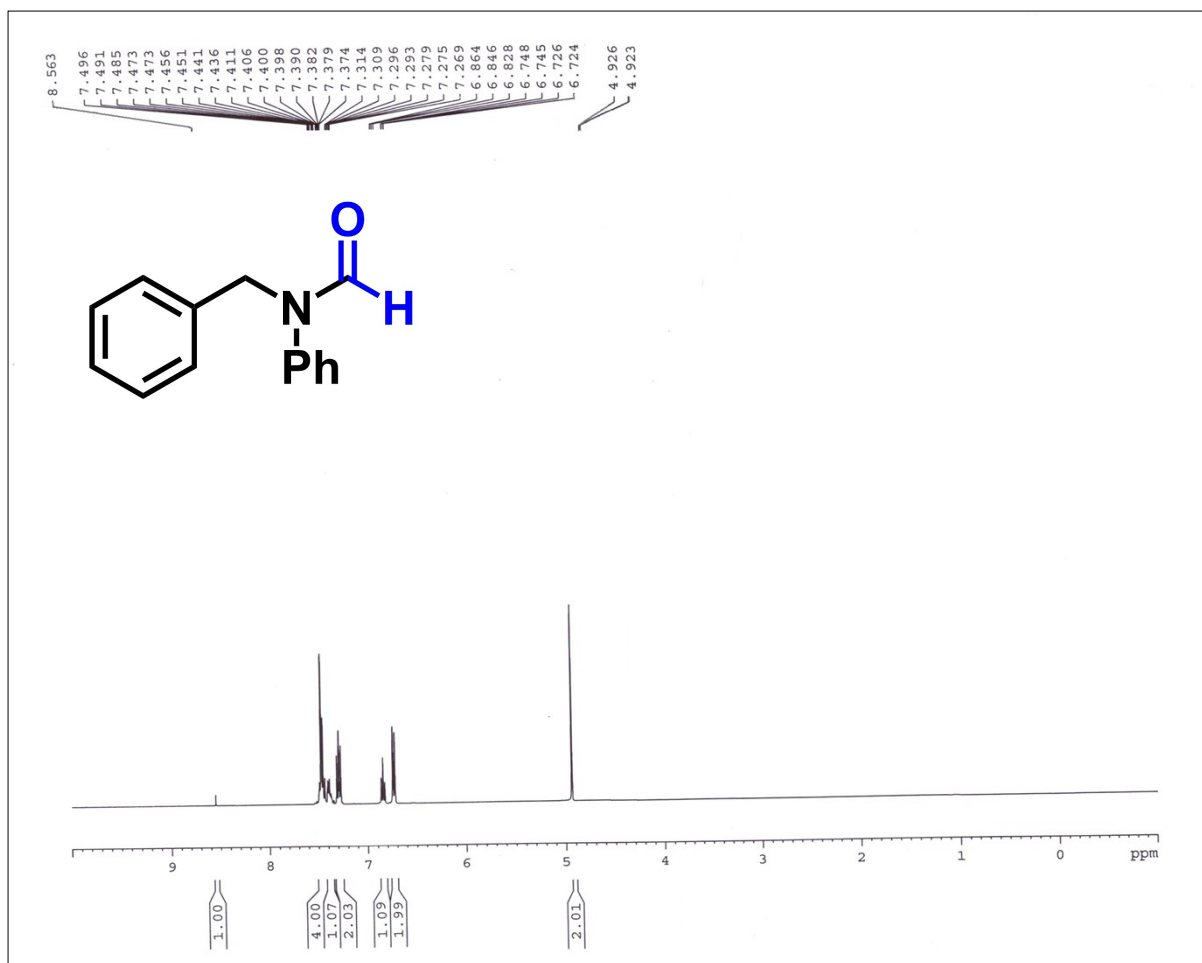


Figure S29: ¹H NMR data of N-phenyl-N-benzyl formamide

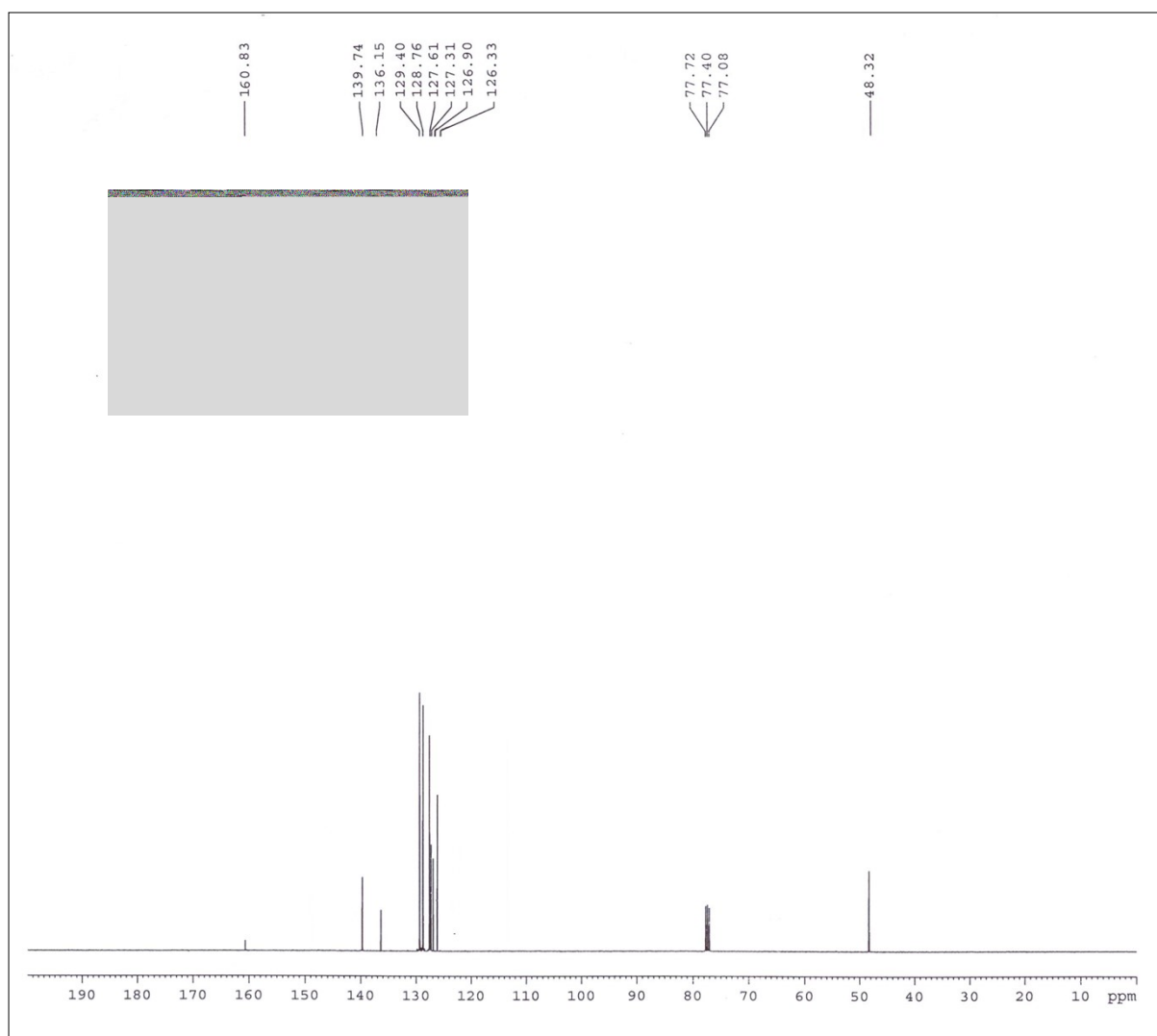


Figure S30: ^{13}C NMR data of N-phenyl-N-benzyl formamide

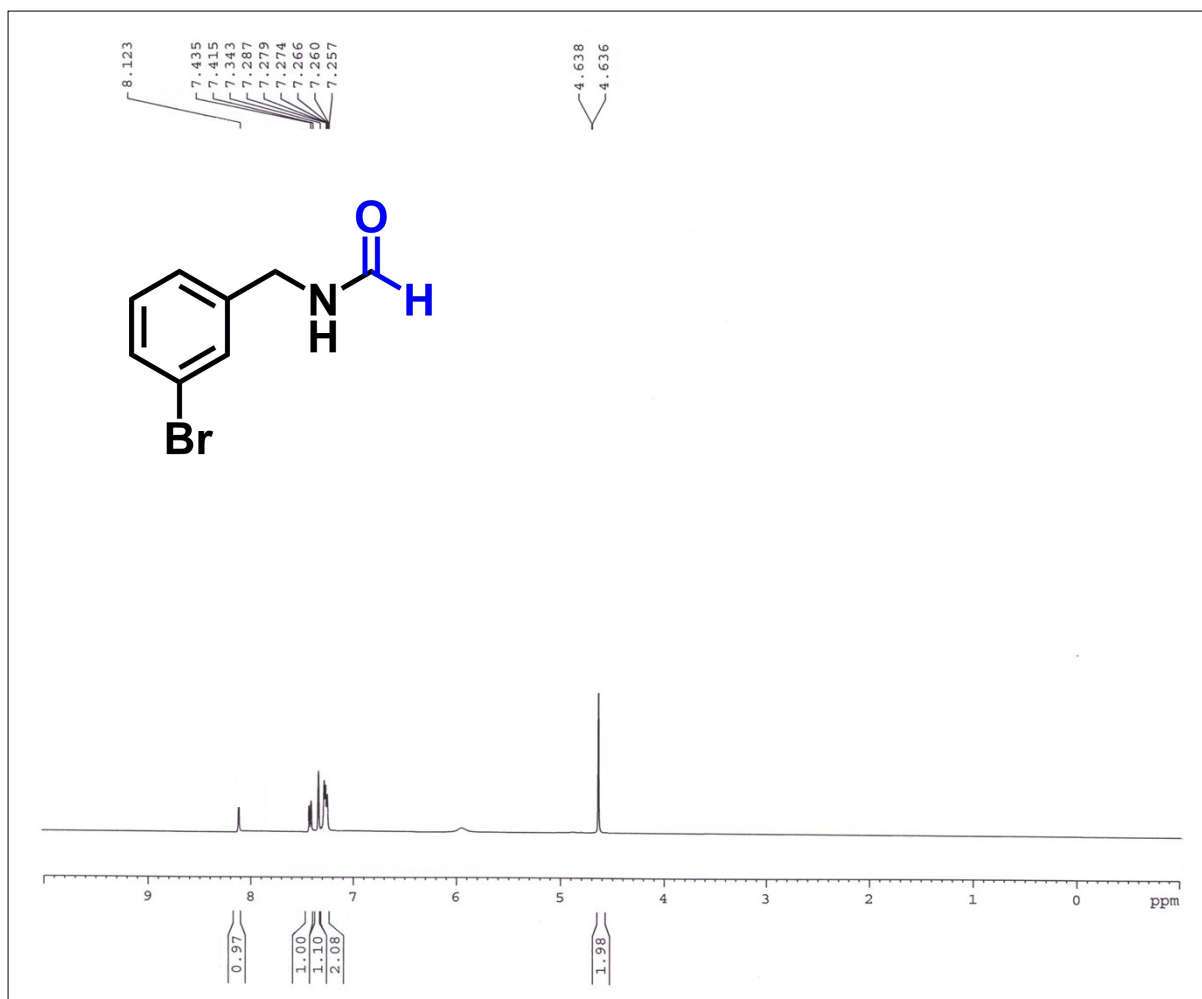


Figure S31: ¹H NMR data of N-(3-bromobenzyl) formamide

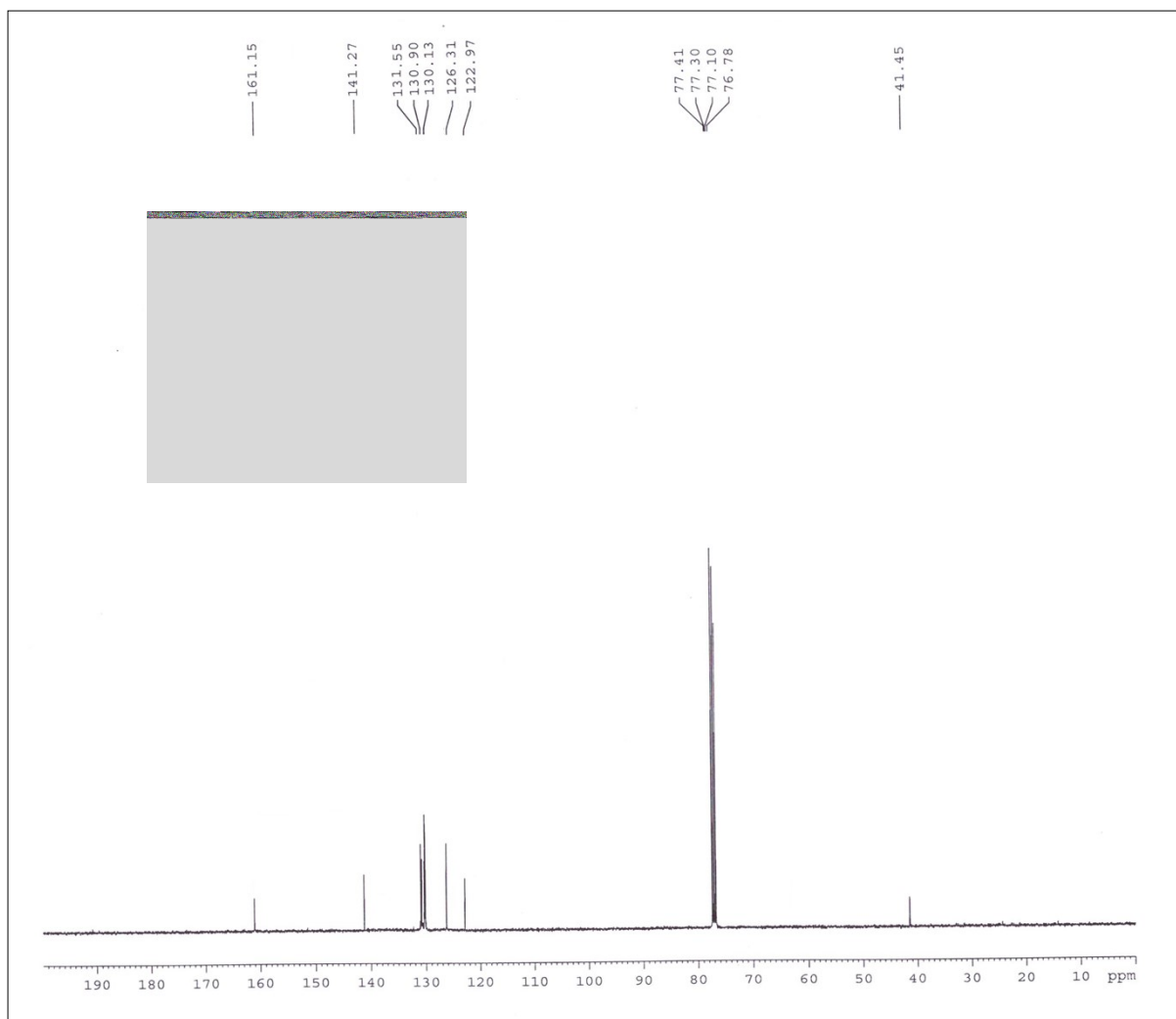


Figure S32: ^{13}C NMR data of N-(3-bromobenzyl) formamide

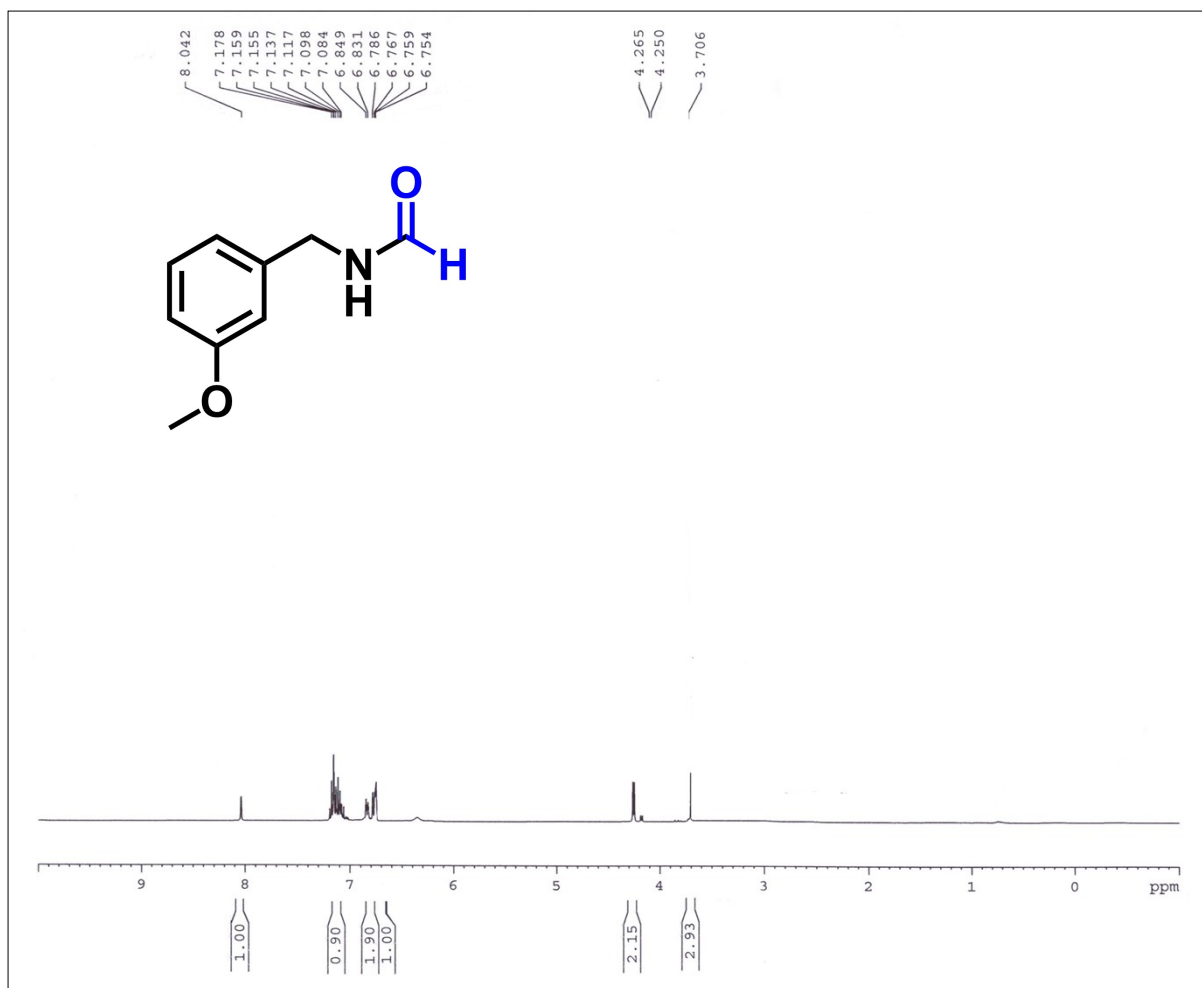


Figure S33: ¹H NMR data of N-(3-methoxybenzyl) formamide

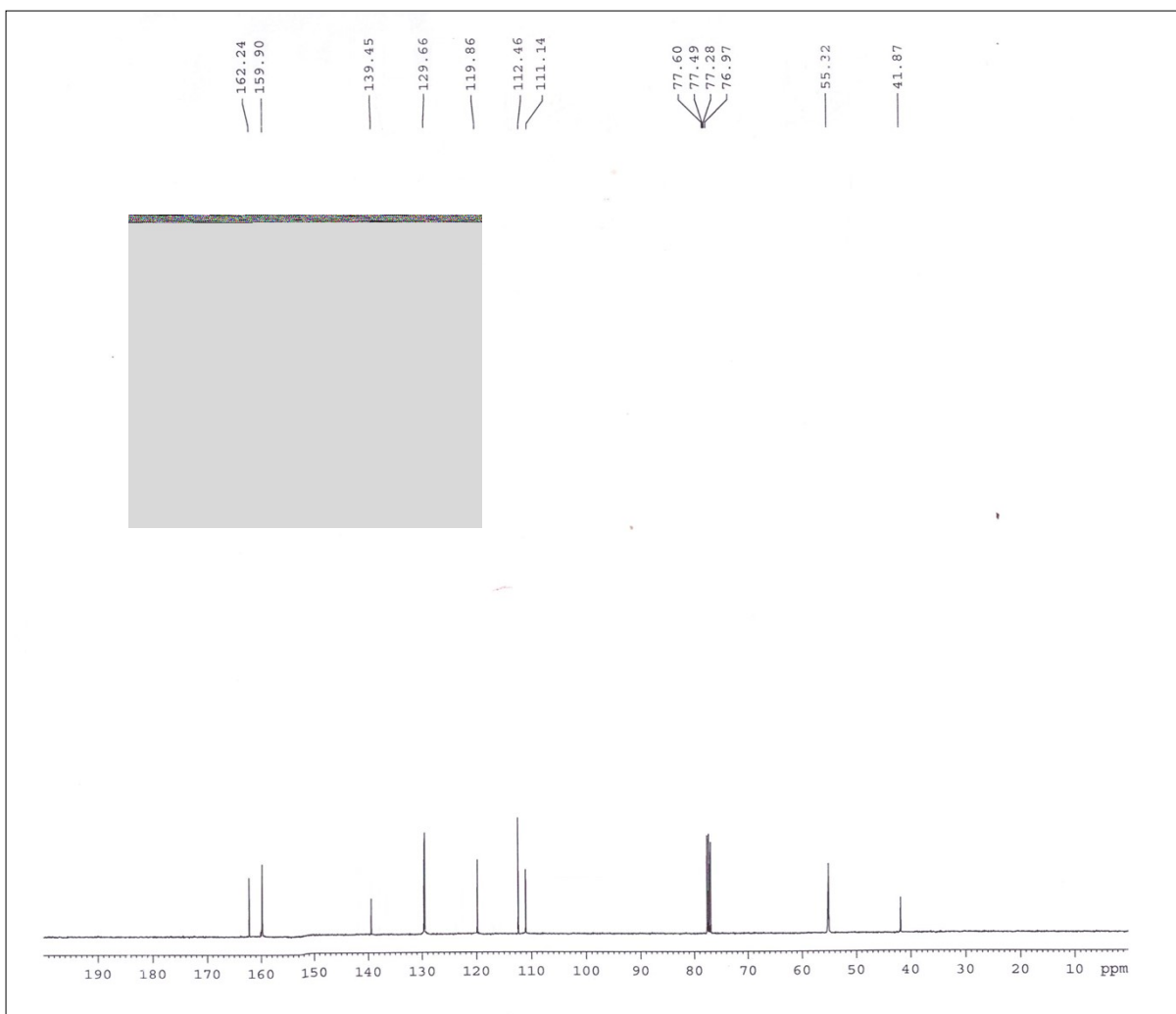


Figure S34: ^{13}C NMR data of N-(3-methoxybenzyl) formamide

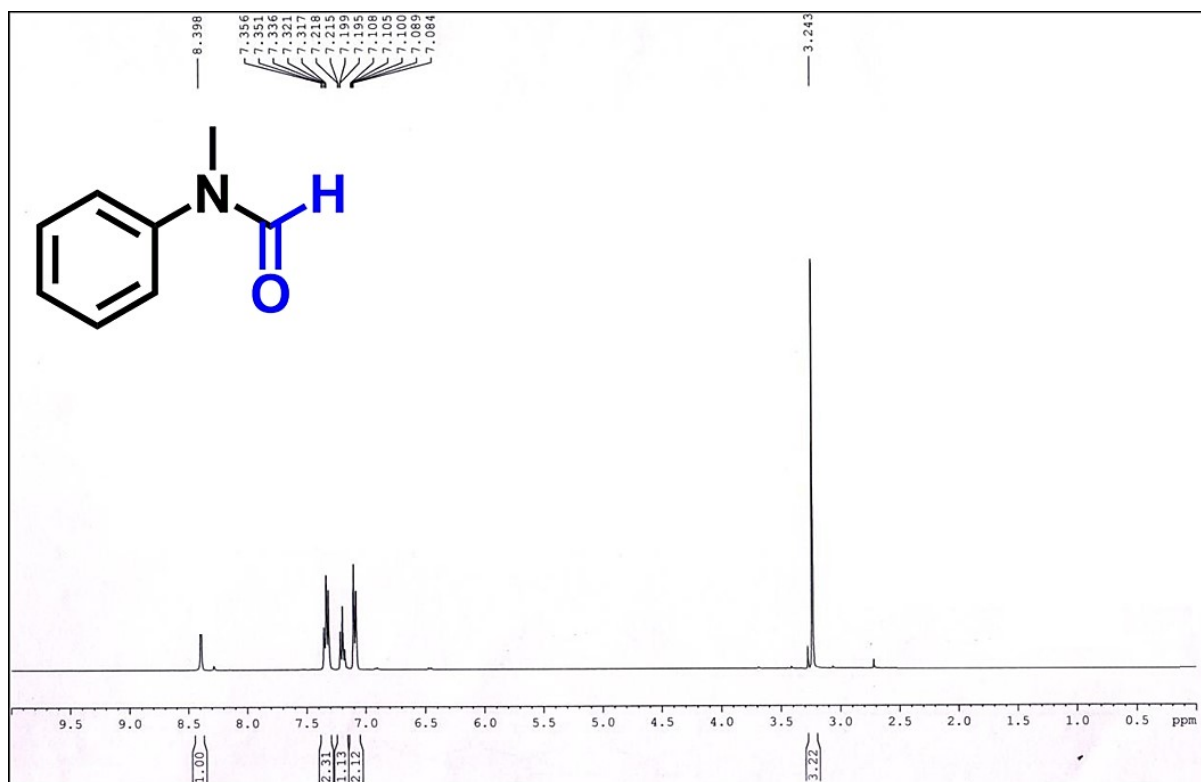


Figure S35: ¹H NMR data of N-methyl-N-phenyl formamide

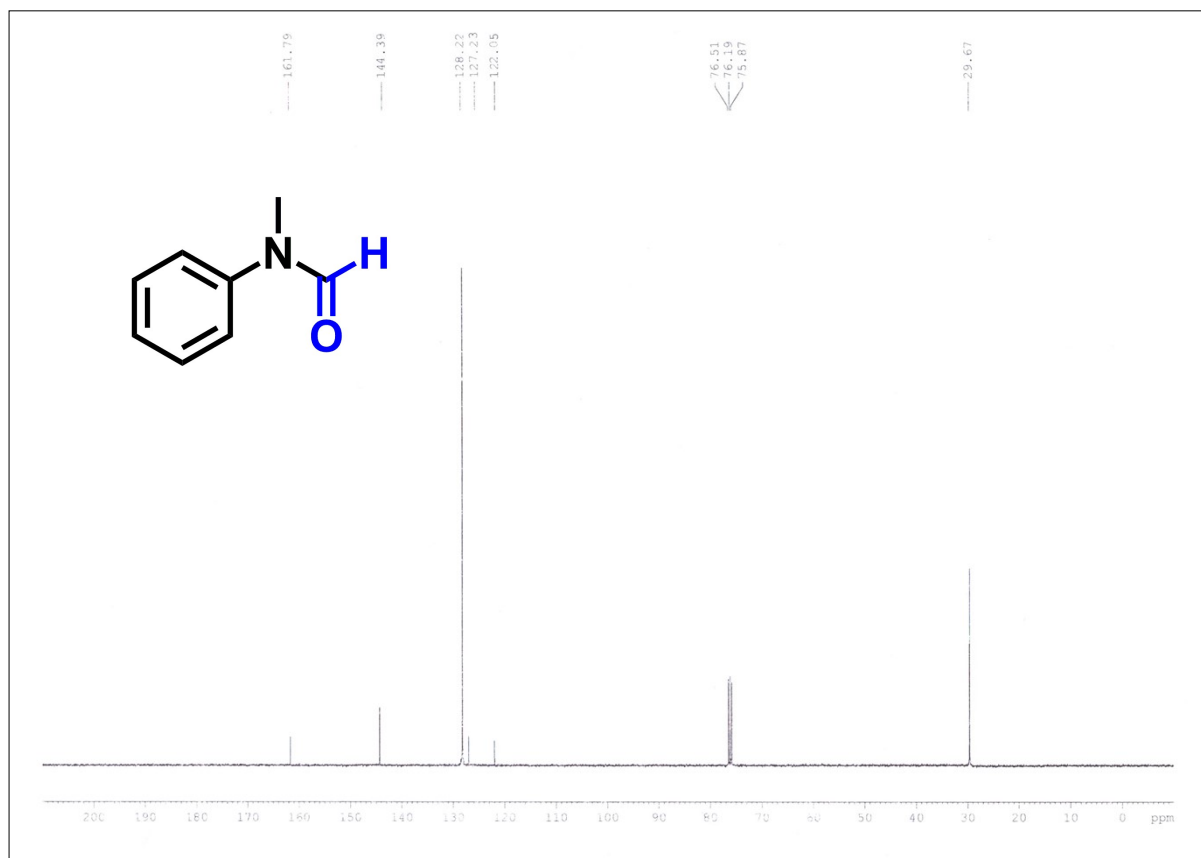


Figure S36: ¹³C NMR data of N-methyl-N-phenyl formamide

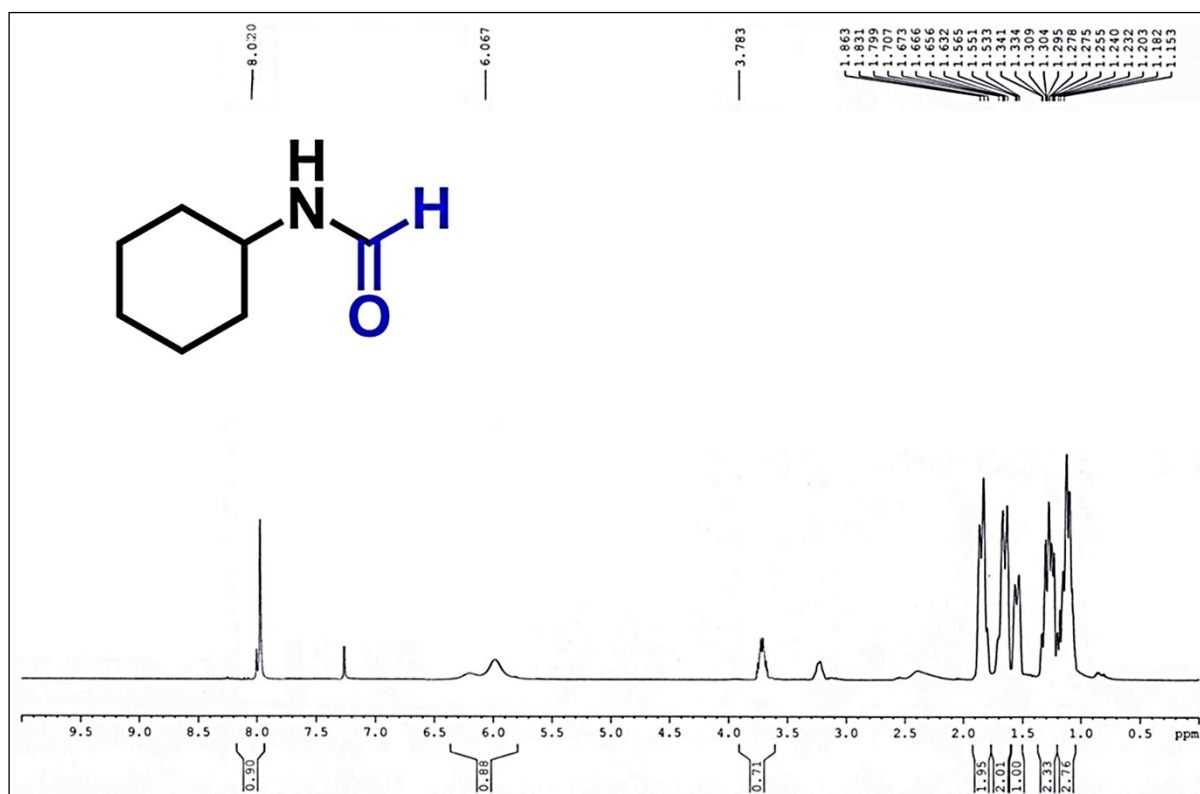


Figure S37: ^1H NMR data of N-cyclohexyl formamide

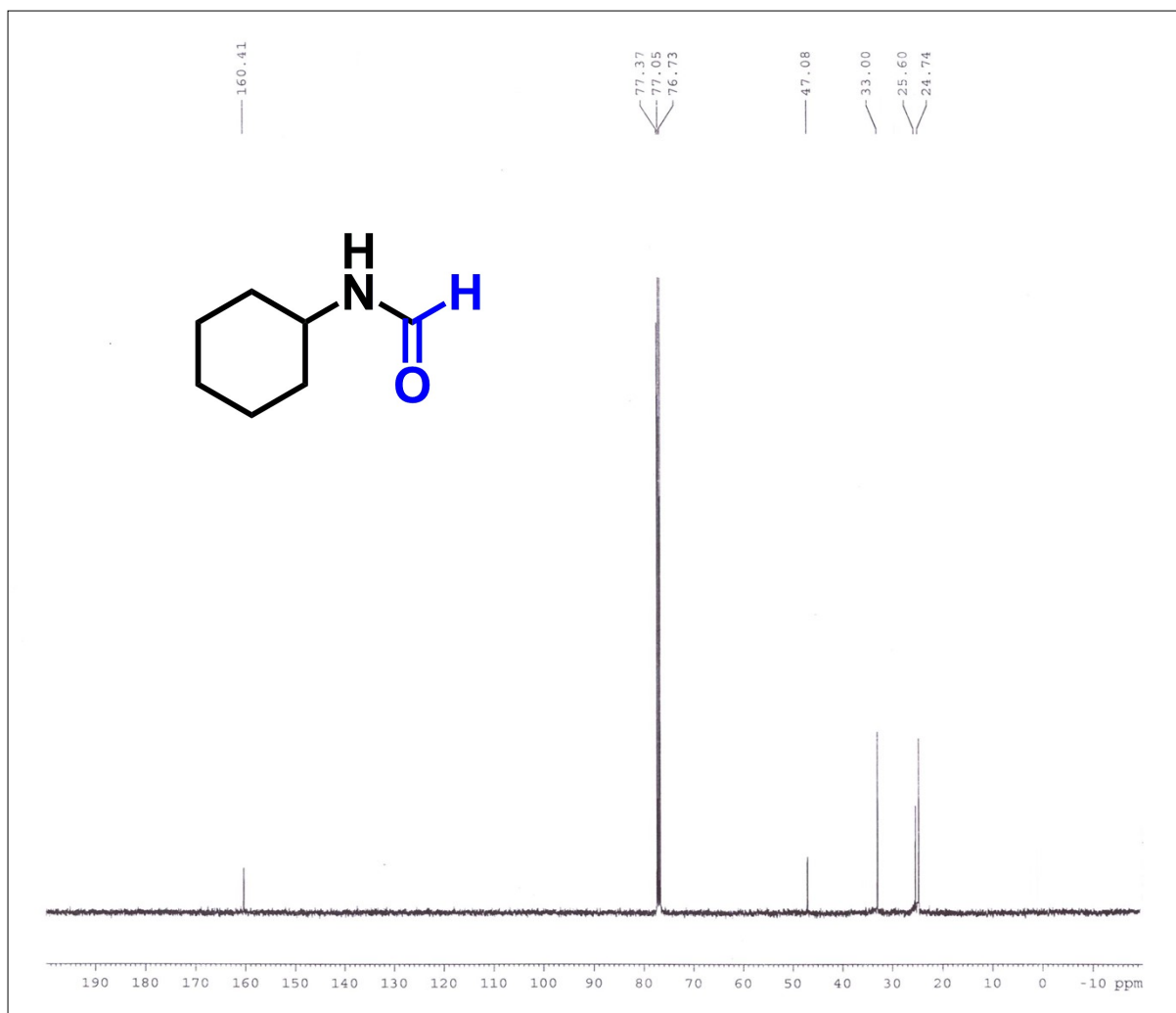


Figure S38: ^{13}C NMR data of N-cyclohexyl formamide

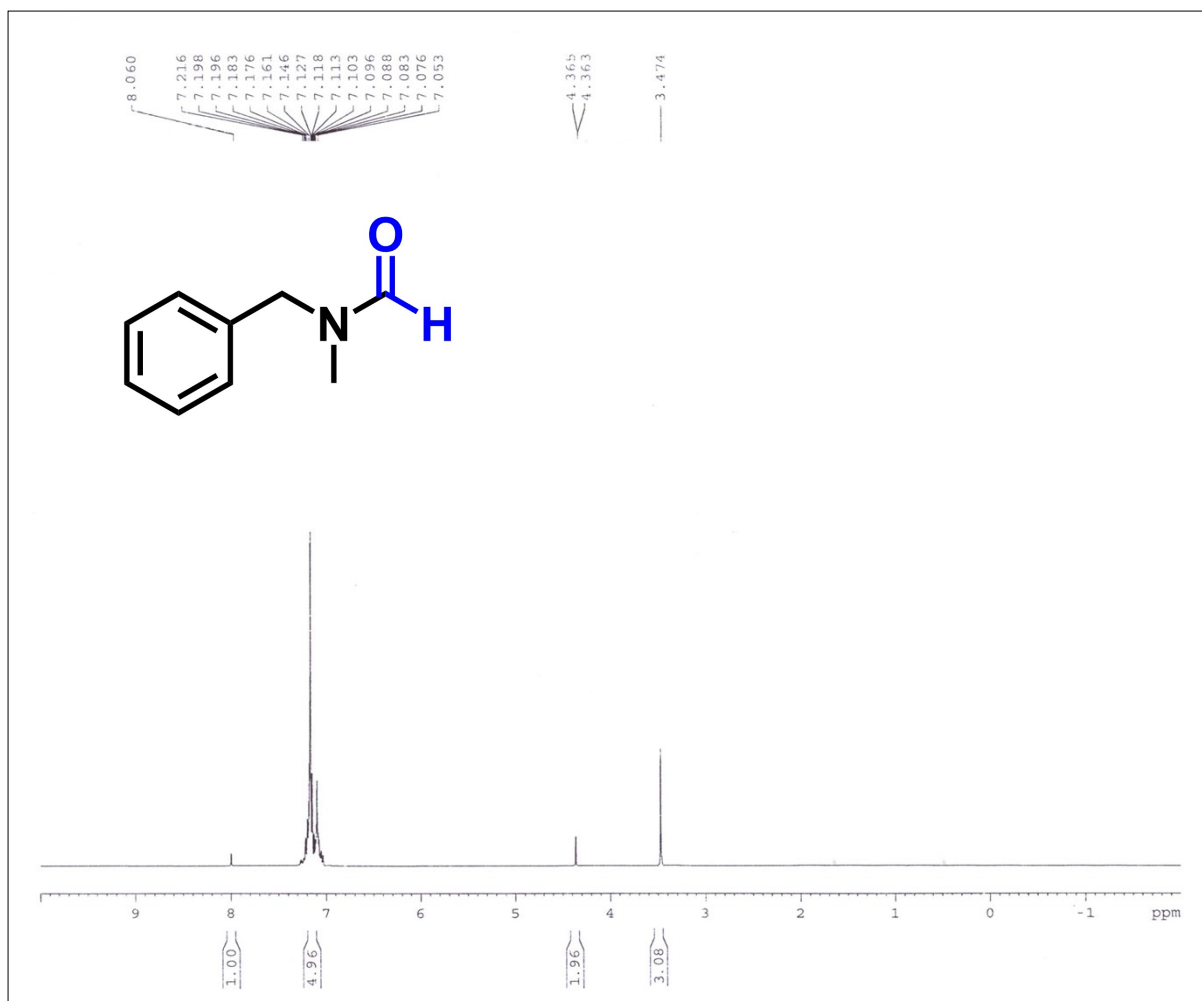


Figure S39: ¹H NMR data of N-methyl-N-benzyl formamide

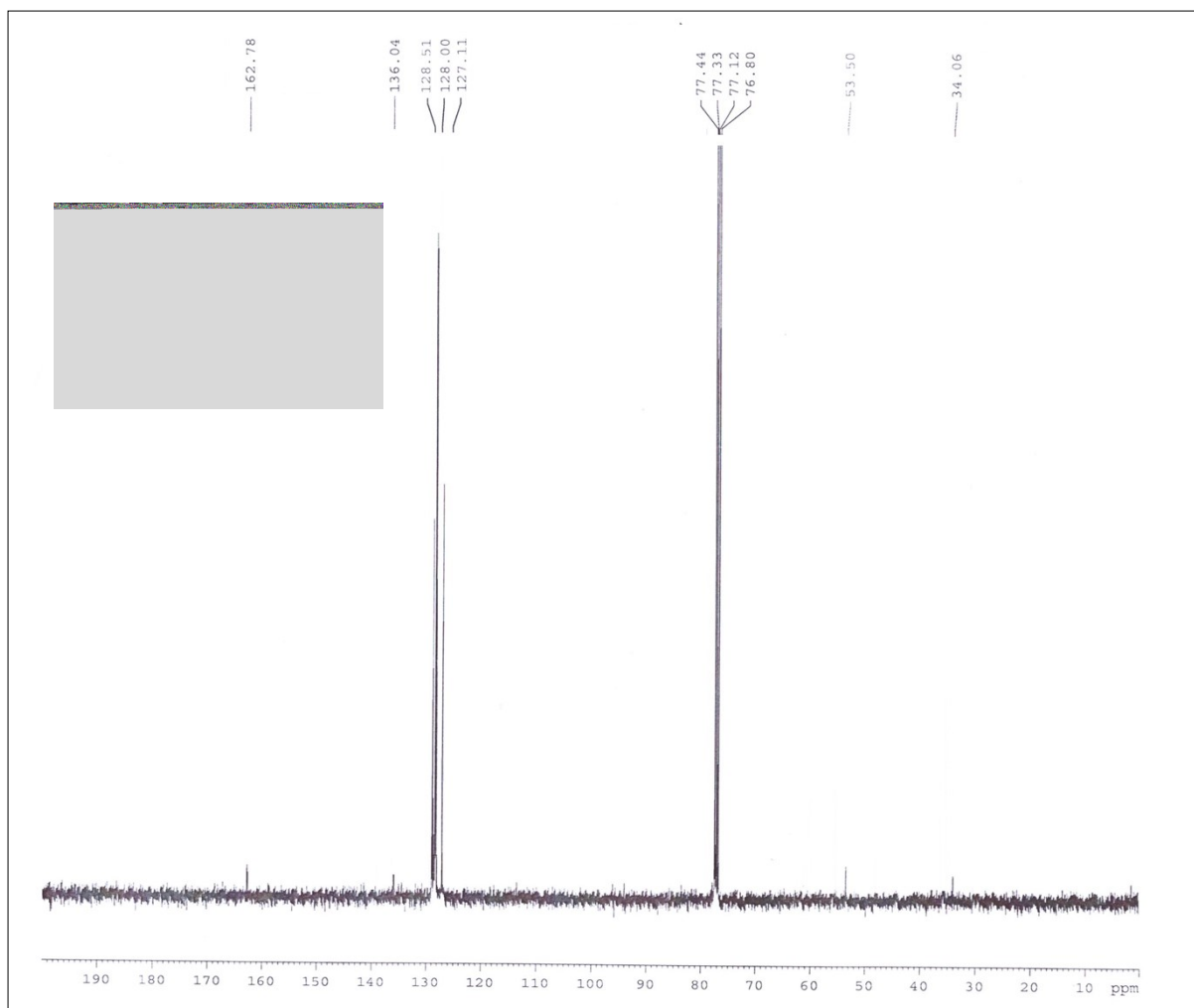


Figure S40: ^{13}C NMR data of N-methyl-N-benzyl formamide

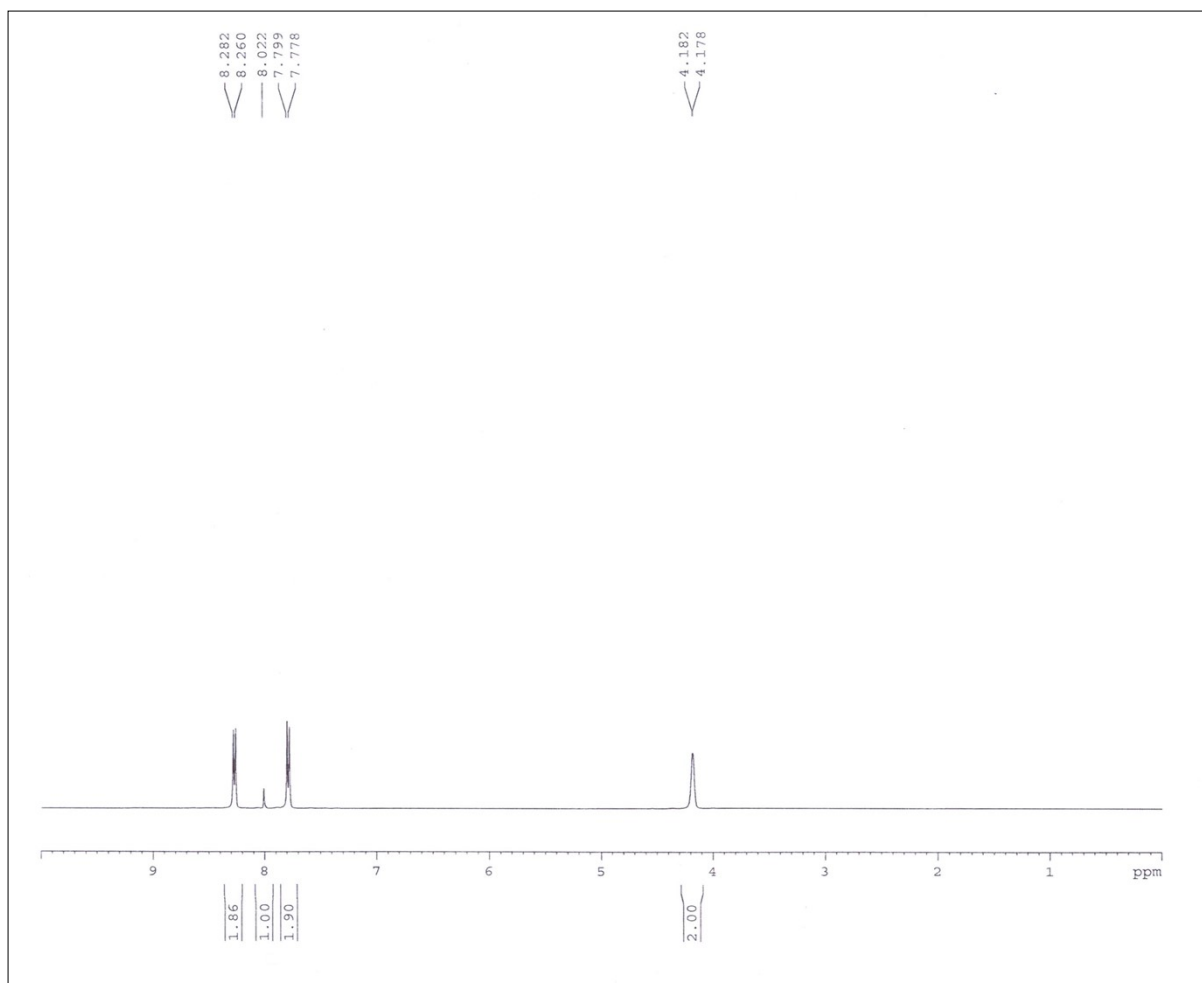


Figure S41: ^1H NMR data of N-(4-nitrobenzyl) formamide

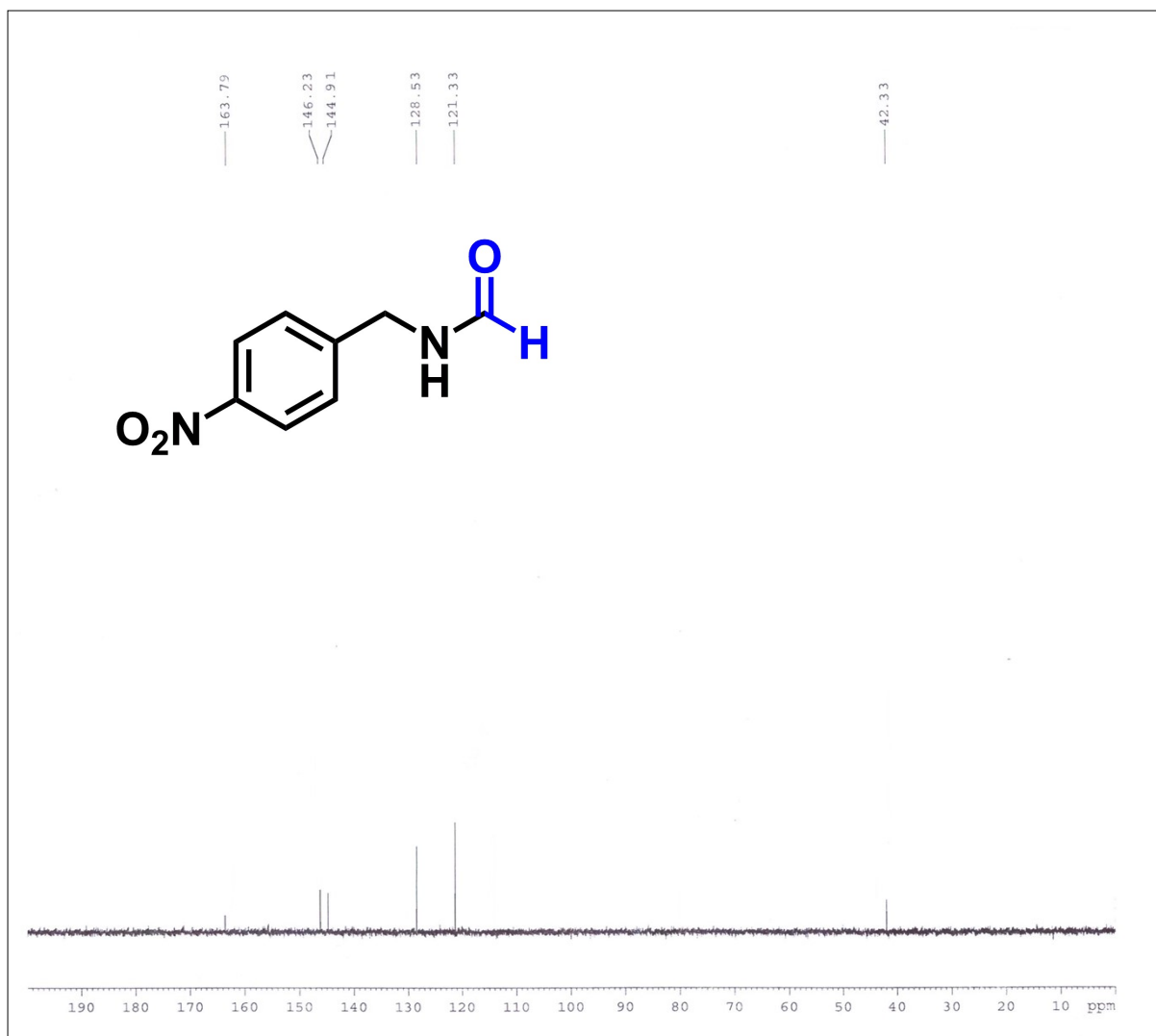


Figure S42: ¹³C NMR data of N-(4-nitrobenzyl) formamide

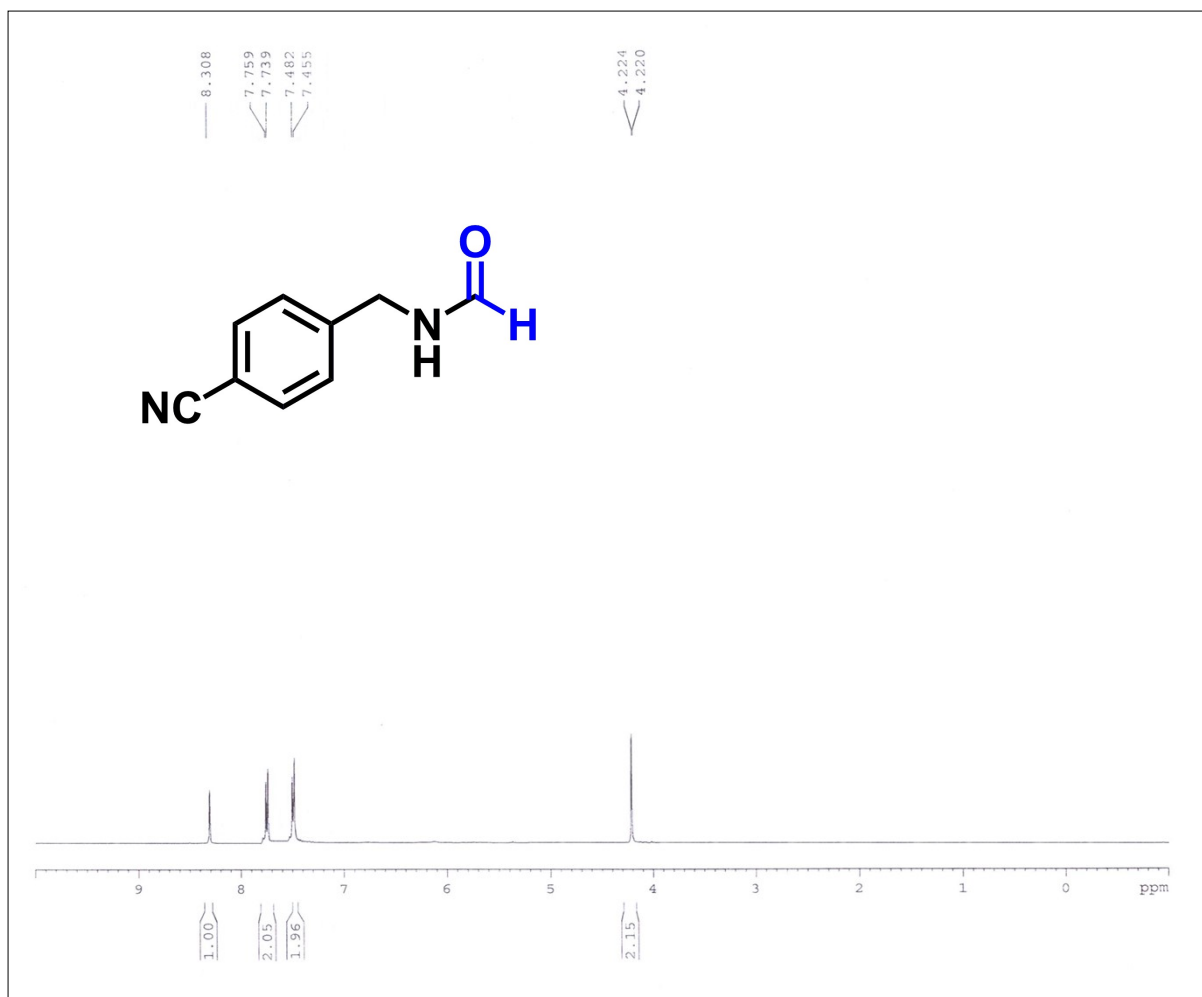


Figure S43: ¹H NMR data of N-(4-cyanobenzyl) formamide

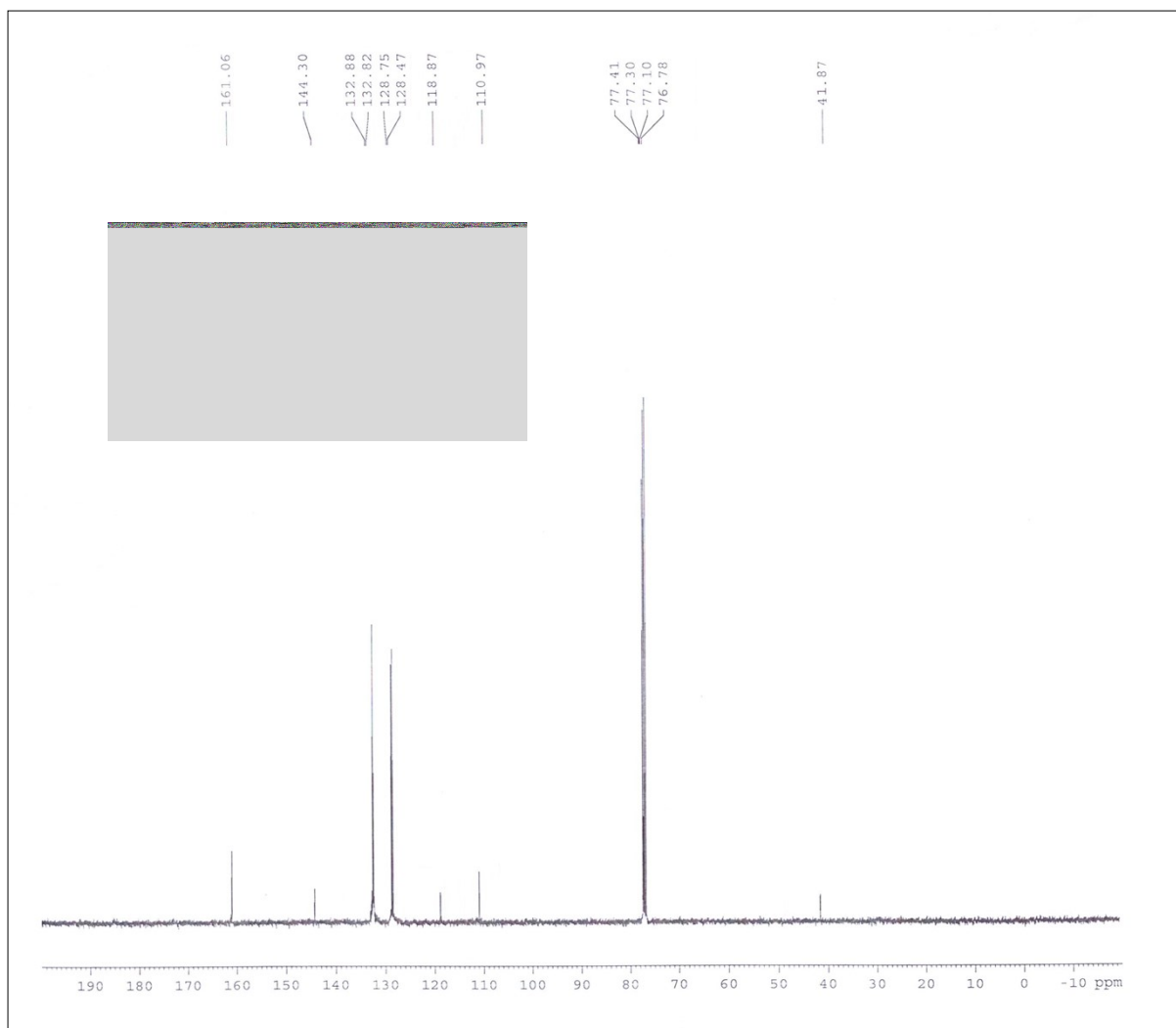


Figure S44: ^{13}C NMR data of N-(4-cyanobenzyl) formamide

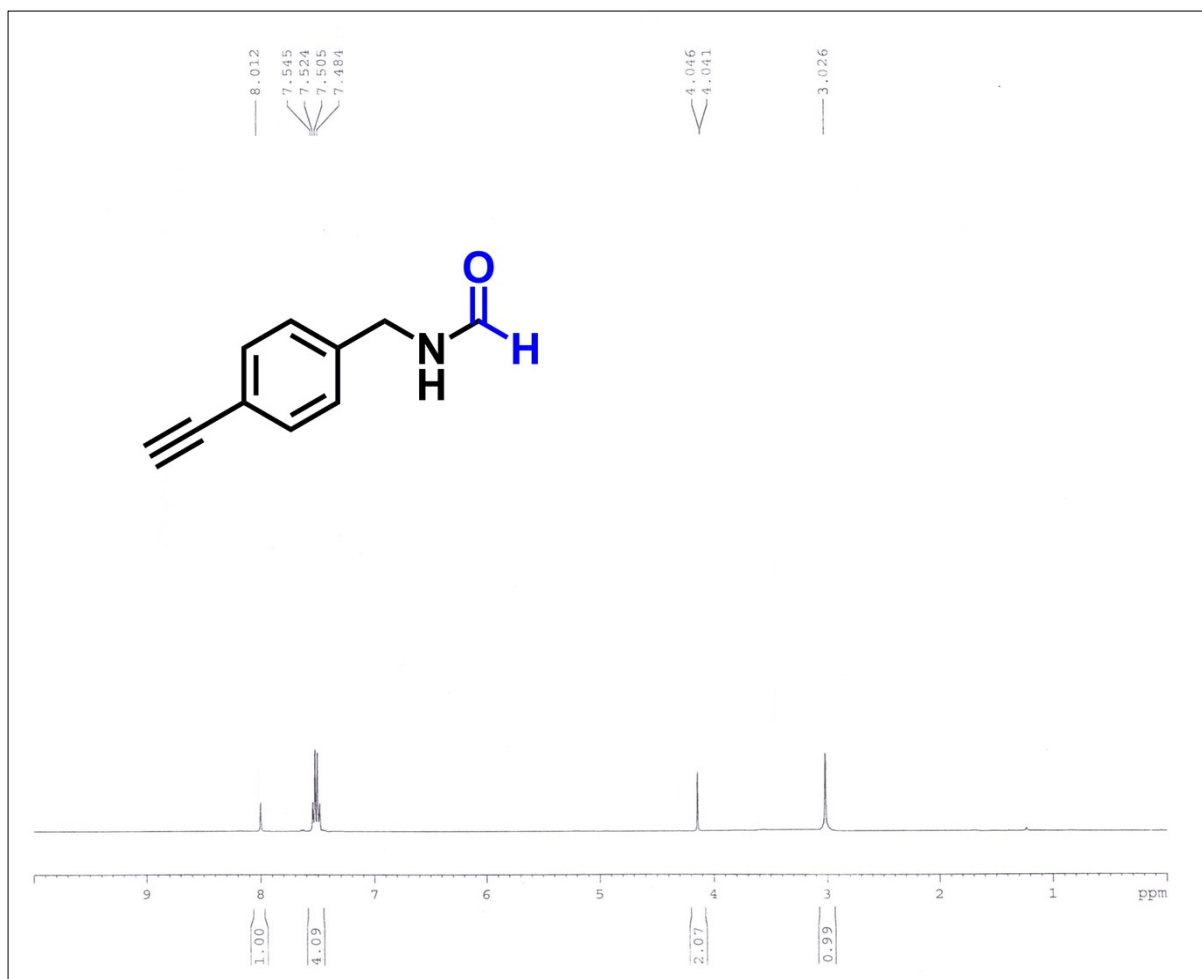


Figure S45: ¹H NMR data of N-(4-ethynylbenzyl) formamide

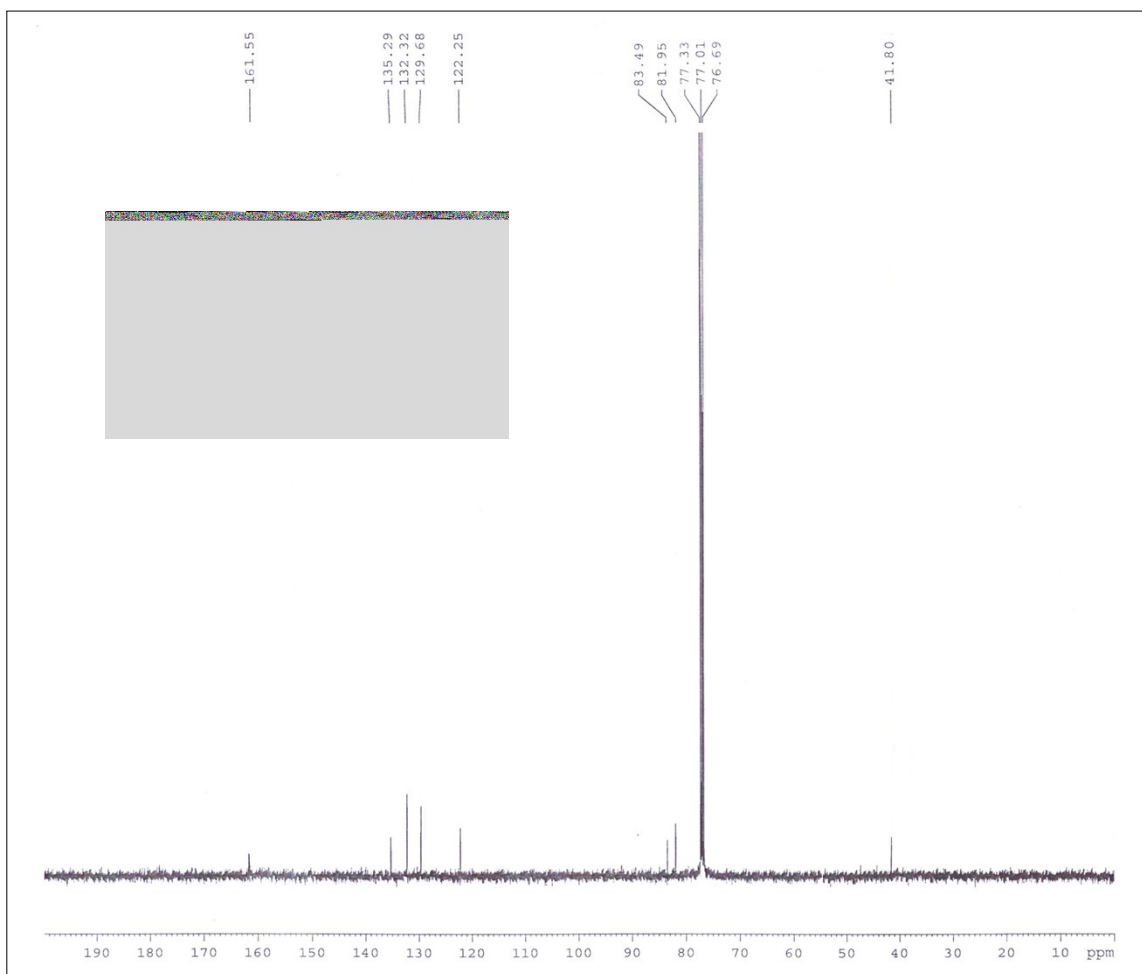


Figure S46: ^{13}C NMR data of N-(4-ethynylbenzyl) formamide

Reference

1. J. H. Chong, M. Sauer, B. O. Patrick, M. J. MacLachlan, Highly stable keto-enamine salicylideneanilines, *Org. Lett.*, 2003, **21**, 3823-3826.
2. B. Kebede, N. Retta, V. J. T. Raju, Y. Chebude, Synthesis and Characterization of 2, 4, 6-tris (hydrazino)-s-triazine and its Metal Complexes. *Transit. Met. Chem.*, 2006, **31**, 19-26.
3. M. Dinari, M. Hatami, Novel N-riched crystalline covalent organic framework as a highly porous adsorbent for effective cadmium removal, *J. Environ. Chem. Eng.*, 2019, **7**, 102907.
4. Z. Wu, Y. Zhai, W. Zhao, Z. Wei, H. Yu, S. Han, Y. Wei, An efficient way for the N-formylation of amines by inorganic-ligand supported iron catalysis, *Green Chem.*, 2020, **22**, 737-741.